

# Towards a categorification of scattering amplitudes

Severin Barmeier<sup>\*1,2</sup>, Prafulla Oak<sup>†3</sup>, Aritra Pal<sup>‡3</sup>, Koushik Ray<sup>§3</sup>, and  
Hipolito Treffinger<sup>¶4</sup>

<sup>1</sup>*Hausdorff Research Institute for Mathematics, Poppelsdorfer Allee 45,  
53115 Bonn, Germany*

<sup>2</sup>*Universität zu Köln, Weyertal 86-90, 50931 Köln, Germany*

<sup>3</sup>*Indian Association for the Cultivation of Science, Calcutta 700 032,  
India*

<sup>4</sup>*Institut de Mathématiques de Jussieu-Paris Rive Gauche, Université de  
Paris, 5 rue Thomas Mann, 75205 Paris, France*

## Abstract

Categorification of scattering amplitudes for planar Feynman diagrams in scalar field theories with a polynomial potential is reported. Amplitudes for cubic theories are directly written down in terms of projectives of hearts of intermediate  $t$ -structures restricted to the cluster category of quiver representations, without recourse to geometry. It is shown that for theories with  $\phi^{m+2}$  potentials those corresponding to  $m$ -cluster categories are to be used. The case of generic polynomial potentials is treated and our results suggest the existence of a generalization of higher cluster categories which we call pseudo-periodic categories. An algorithm to obtain the projectives of hearts of intermediate  $t$ -structures for these types is presented.

---

\*s.barmeier@gmail.com

†prafullaoakwork@gmail.com

‡intap@iacs.res.in

§koushik@iacs.res.in

¶treffinger@imj-prg.fr

# 1 Introduction

The ABHY scheme [1] and the upsurge of activities it initiated unravelled novel connections between the quantum field theoretic computation of scattering amplitudes and a variety of mathematical notions and techniques. The ABHY programme provided a geometric way of writing scattering amplitudes of a biadjoint cubic scalar field theory in four dimensions as the volume form of the dual to the associahedron, a polyhedron associated to the combinatorics of grouping the scattering particles according to the vertices of Feynman diagrams they give rise to. This relationship between the scattering amplitudes and the associahedron led to the connection of the former with the algebraic geometry of Grassmannians, tropical geometry [2], cluster algebras [3,4] and representation theory of quivers and related subjects [5]. The ABHY scheme has been generalized in various directions. In one line of development scalar field theories with higher order interactions were studied [6–11]. Another class of generalization is to obtain similar pictures for higher loop Feynman diagrams [12–14].

Various aspects of combinatorial computations are succinctly described within the framework of homological algebra using triangulated categories of quiver representations and related ideas. In an attempt to categorify the computation of scattering amplitudes it has been shown that the scattering amplitude can be written down directly for a cubic scalar field theory from the cluster category of type  $A$  quivers. In order to obtain the canonical form of  $N$ -particle scattering in a cubic scalar field theory one writes the cluster category of the  $A_{N-3}$  quiver. The planar variables appearing in the different terms of the canonical form are obtained as the mass (modulus) of the central charges of the summands of cluster tilting objects, or equivalently central charges of projectives of intermediate  $t$ -structures in the corresponding derived category [15].

In the present article we complete the categorification of scattering amplitudes of tree-level planar Feynman diagrams for arbitrary polynomial potentials. The scattering amplitude of  $N$  scalars in a  $\phi^{m+2}$  theory for any integral  $m$  corresponding to such diagrams with  $n$  vertices of valency  $m$  is written in terms of the  $m$ -cluster tilting objects of an  $A_{n-1}$  quiver, where  $N = mn + 2$ , specifically, in terms of projectives of the hearts of the  $m$ -intermediate  $t$ -structures of the corresponding derived category. Generalizing further, the amplitude for a theory with potential  $\sum_i \lambda_i \phi^{m_i+2}$ , where the sum is assumed to be over a finite number of terms, is written in terms of projectives of hearts in the intermediate  $t$ -structures restricted to what we call here a pseudo-periodic category, corresponding to the  $N$ -periodic triangulated thick subcategory of the derived category of an  $A_{n-1}$  quiver, where  $n = \sum_i n_i$  and  $N = \sum_i m_i n_i + 2$ . This yields the amplitude for planar Feynman diagrams with  $n_i$  vertices of valency  $m_i + 2$ , with a total number of  $n$  vertices. One of the major motivations for the categorical approach is to facilitate effective bookkeeping, although this approach appears to indicate more. The pseudo-periodic category, which the form of scattering amplitudes suggests is novel and has not been studied earlier. All this is based on the relations between planar Feynman diagrams, polygons dual to them, their subdivisions and the connection of these to the representation theory of quivers, uncovered in previous studies.

In section 2 we recall some of the known features which lead to the categorification using some examples. In section 4 we shall demonstrate how the categorical picture yields

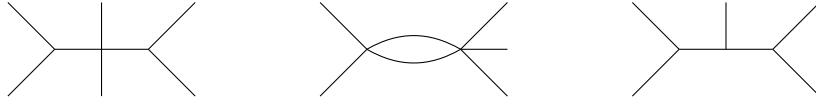


Figure 1: Planar Feynman diagrams

the amplitude directly from the field theoretic specification, after recalling the pertinent notions in section 3.

## 2 Planar diagrams, angulations of polygons and meshes

Let us begin with the planar Feynman diagrams of  $N$ -particle scattering in an interacting scalar field theory with a potential polynomial in the field  $\phi$ ,

$$V(\phi) = \sum_i \lambda_{m_i+2} \phi^{m_i+2}, \quad (1)$$

where the  $m_i$ 's are a finite set of positive integers and  $\lambda_i$  is the coupling at an interaction vertex of valency  $m_i + 2$ . The diagrams have  $N$  external legs, satisfying

$$N = \sum_i m_i n_i + 2 - 2L, \quad (2)$$

where  $n_i$  denotes the number of (internal) vertices in the diagram with valency  $m_i + 2$  and  $L$  denotes the number of internal loops. This can be seen from the Euler characteristic of a planar graph with  $V$  number of vertices,  $E$  number of edges and  $F$  faces, namely,

$$V - E + F = 2. \quad (3)$$

We have  $V = N + \sum_i n_i$  vertices in a planar Feynman diagram,  $N$  being the number of monovalent vertices corresponding to the external legs. The total number of edges is given by  $2E = \sum_{i \neq 2} i V_i$ , for  $V_i$  number of vertices with valency  $i$  in a graph. For the planar Feynman diagrams, this becomes

$$2E = N + \sum_i (m_i + 2) n_i. \quad (4)$$

Also, counting the unbounded face in the plane as one, the total number of faces is one more than the number of loops,  $F = 1 + L$ . Plugging these expressions into (3) we obtain (2). Some examples are shown in Fig 1. The leftmost Feynman diagram has two vertices of valency 3 and one of valency 4. Thus,  $m_1 = 1$ ,  $n_1 = 2$ ,  $m_2 = 2$ ,  $n_2 = 1$  and no loop, accounting for the number of external particles  $N = 6$  by (2). The middle one has one vertex of valency 4, one of valency 5 and one loop. Thus,  $m_1 = 2$ ,  $m_2 = 3$ ,  $n_1 = n_2 = 1$ , and  $L = 1$ , leading to  $N = 5$  external particles. In the special cases where the potential  $V(\phi)$  has a single term, the Feynman diagrams have vertices of one type, with a fixed valency as indicated in the last diagram with  $m = 1$ ,  $n = 3$ ,  $L = 0$ ,  $N = 5$ .

Let us point out that in the special case of a cubic theory the 1-loop diagrams have  $N = n$  by (2). These may be related to the cluster category of  $D_n$  quivers [14]. However,

the  $m$ -cluster category of  $D_n$  quivers are described in terms of  $m$ -angulations of a polygon with  $(mn - m + 1)$  sides [16]. This number matches (2) with  $L = 1$  only if  $m = 1$ . Thus, the analogy with  $D_n$  quivers may not hold beyond the cubic theory.

From now on we shall refer to the planar tree-level Feynman diagrams, that is the ones with no loops,  $L = 0$ , as planar diagrams, unless otherwise qualified. For the planar diagrams (2) reads

$$N = \sum_i m_i n_i + 2. \quad (5)$$

Let us also define the total number of vertices,

$$n = \sum_i n_i. \quad (6)$$

A planar diagram for an  $N$ -particle scattering amplitude is dual to a decomposition of an  $N$ -gon by polygons with lesser number of sides. We shall refer to such a subdivision of a polygon as an angulation. The internal lines of an angulation are referred to as diagonals. If the angulation is with polygons all of which have the same number of sides, say  $m$ , it is called an  $m$ -angulation. The number of edges of an internal polygon in an angulation is equal to the valency of lines at a vertex of the Feynman diagram, the vertex being associated with the interior of the polygon. This is indicated in Fig. 2. The graphical

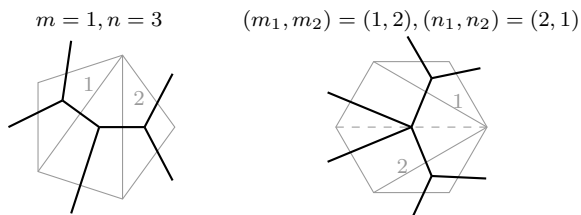


Figure 2: Angulation of polygons and Feynman diagrams

connection between planar diagrams and angulation of polygons is algebraically realised by introducing the so-called planar variables. Indeed, the scattering amplitude is expressed in terms of these Lorentz invariant combinations of momenta of the external particles. We briefly recall the definition of kinematic variables for the scattering of a system of  $N$  scalar particles [1]. The momenta of such particles are vectors in  $\mathbf{R}^{1,3}$ , denoted  $\mathbf{p}_i$  for  $i = 1, \dots, N$  which satisfy the conservation equation

$$\sum_{i=1}^N \mathbf{p}_i = 0. \quad (7)$$

This equation can be solved by writing the momenta  $\mathbf{p}$  in terms of another set of  $N$  four-vectors  $\mathbf{x}$  defined via

$$\mathbf{p}_i = \mathbf{x}_{i+1} - \mathbf{x}_i, \quad (8)$$

where the indices of  $\mathbf{x}$  are defined modulo  $N$ , in particular,  $\mathbf{x}_{N+1} = \mathbf{x}_1$ . Quadratic invariants in momenta for a pair of particles furnish the Mandelstam variables

$$s_{ij} = (\mathbf{p}_i + \mathbf{p}_j)^2, \quad (9)$$

where the norm of a four-vector  $\mathbf{p} = (p^0, p^1, p^2, p^3)$  is defined as  $\mathbf{p}^2 = -(p^0)^2 + (p^1)^2 + (p^2)^2 + (p^3)^2$ . The planar variables are quadratic invariants defined similarly with  $\mathbf{x}$ 's, namely,

$$X_{i,j} = (\mathbf{x}_i - \mathbf{x}_j)^2. \quad (10)$$

The indices are symmetric by definition, that is,  $X_{j,i} = X_{i,j}$ . Throughout this article we write the planar variables  $X_{i,j}$  with subscripts ordered as  $i < j$ . The planar variables are related to the Mandelstam variables by

$$s_{ij} = \mathbf{p}_i^2 + \mathbf{p}_j^2 + X_{i,j+1} + X_{i+1,j} - X_{i,j} - X_{i+1,j+1}, \quad (11)$$

as can be derived from the definitions. If we further assume that the particles are massless, that is, their momentum vectors are null,  $\mathbf{p}_i^2 = 0$  for each  $i$ , then

$$s_{ii} = 2\mathbf{p}_i^2 = 0, \quad X_{i,i+1} = \mathbf{p}_i^2 = 0, \quad (12)$$

and the relation (11) becomes

$$s_{ij} = X_{i,j+1} + X_{i+1,j} - X_{i,j} - X_{i+1,j+1}. \quad (13)$$

The right-hand side is seen to coincide with the negative discrete Laplacian operating on the planar variables. Some of the planar variables vanish by definition,

$$\begin{aligned} X_{N,N+1} = X_{N,1} = X_{1,N} = 0, \\ X_{2,N+1} = X_{2,1} = X_{1,2} = 0. \end{aligned} \quad (14)$$

Plotting  $N$  points on the plane, each for an  $x_i$ , joined by edges corresponding to the null variables (14) yields a polygon. The non-vanishing  $X_{i,j}$  are then identified with the diagonals of angulations of the polygon, as shown for example, in Fig 3. This is the dual picture of planar diagrams described above. Quadratic invariants with more than a pair of particles are defined as

$$s_{k_1 k_2 \dots k_n} = \left( \sum_{i=1}^n \mathbf{p}_{k_i} \right)^2, \quad \forall i, k_i \in \{1, \dots, N\}. \quad (15)$$

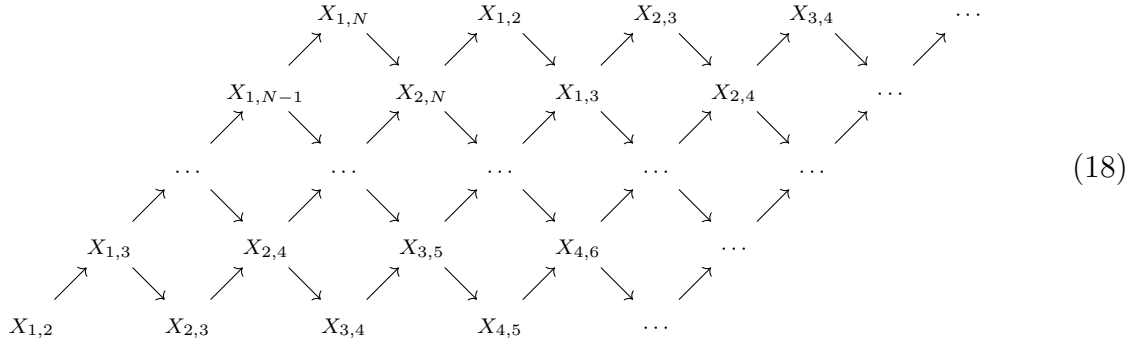
Many of these multi-indexed variables are related by momentum conservation (7). For example, for  $N = 5$  we have  $s_{123} = s_{45}$ . These are related to the planar variables as

$$X_{i,j} = s_{i+1 \dots j-1}. \quad (16)$$

For a given  $N$  and a potential (1) a mesh diagram is obtained without alluding to the angulations. The discrete Laplacian (13) is pictorially represented as

$$s_{ij} = \begin{array}{ccc} & X_{i,j+1} & \\ & \nearrow \quad \searrow & \\ X_{i,j} & & X_{i+1,j+1} \\ & \searrow \quad \nearrow & \\ & X_{i+1,j} & \end{array} \quad (17)$$

For a given value of  $N$ , this unit can be woven into a mesh which has the form [14]



The top and the bottom rows are void, due to (12) and (14), the corresponding  $X$ 's being null. Discarding these rows we obtain a mesh of  $X$ 's with arrows. This is the mesh diagram for a  $\phi^3$  theory with  $m = 1$ . However, including the rows of null planar variables in the bottom and top is convenient for weaving the mesh, especially for the general cases. Let us also point out that due to the periodicity of the indices such a mesh is always finite.

For  $\phi^{m+2}$  theories, or, more generally for theories with a generic polynomial potential (1), the knitting algorithm to obtain the mesh diagram of planar variables is to be modified. Instead of the discrete Laplacian, the basic unit is taken to be [12]

$$S_{ij}^{m,m'} := \sum_{k'=0}^{m'-1} \sum_{k=0}^{m-1} s_{i+k,j+k'} = X_{i,j+m'} + X_{i+m,j} - X_{i,j} - X_{i+m,j+m'} \quad (19)$$

for a given pair  $(m, m')$ . This is represented pictorially as

to be knit into a mesh.

Weaving these units into a mesh diagram is rather cumbersome. Significant simplification is achieved by noting that the planar variables appearing in the mesh are the diagonals of angulations of polygons. While a planar diagram of the cubic theory is dual to a triangulation, which is a maximal subdivision of a polygon, the diagrams in theories with higher indices of  $\phi$  correspond to angulations with polygons having number of sides more than three. These can be obtained by starting with the triangulation and then systematically omitting diagonals, leaving a subset. For example, the angulation of the polygon described in the right in Fig. 2 can be obtained by deleting the dashed diagonal from the triangulation of the polygon. While enumeration of these angulations is cumbersome, it translates to a combinatorial algorithm in terms of the mesh, which we proceed to describe.

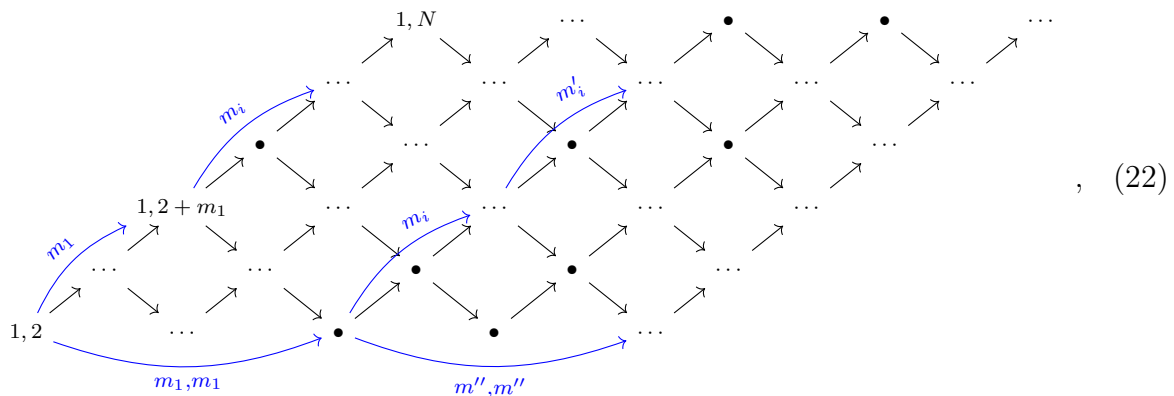
Starting from the mesh (18) corresponding to triangulations, entries are to be deleted to obtain the mesh for theories with general polynomial potentials. Given the number of vertices  $n_i$  with valency  $m_i$  in a planar diagram we first write a partition of the number  $\sum_i m_i n_i = N - 2$  such that  $m_i$  appears  $n_i$  number of times, namely,

$$\Lambda = (\overbrace{m_1, \dots, m_1}^{n_1 \text{ times}}, \overbrace{m_2, \dots, m_2}^{n_2 \text{ times}}, \dots, \overbrace{m_i, \dots, m_i}^{n_i \text{ times}}, \dots). \quad (21)$$

All permutations of the partition correspond one-to-one with the planar diagrams of a certain order in the couplings. Planar variables are then picked from the mesh (18) using  $\Lambda$  by going over the slices beginning with the first one starting at  $X_{1,2}$  according to the rules,

1. on a slice the entries obtained by incrementing the second index  $j$  of  $X_{i,j}$  are collected into a smaller slice, keeping their order
2. successive slices are chosen by adding  $m_i$  from the partition to both indices of the bottom row and shifting entries of  $\Lambda$  periodically by one place
3. the above two steps are continued until the first slice is repeated.

This is pictorially depicted as



where only the indices  $i, j$  of  $X_{i,j}$  are marked in the mesh diagrams, a convention followed in the sequel. A concrete example of this procedure, which is more easier done than said, is discussed in Example 3. Let us hasten to add that for a potential (1) with a single term  $\phi^{m+2}$ , the procedure is extremely simple. Starting with the first slice of (18), slices are selected in steps of  $m$  and entries of each of these are collected in steps of  $m$  starting with the null entry in the bottom row.

Enumeration of *all* the angulations of  $N$ -gons and keeping track of these in deriving the amplitude turns out to be as difficult a bookkeeping problem as drawing all the Feynman diagrams. In the categorical approach developed here it is possible to start from the combinatorics of the mesh diagram obtained using the properties of the planar variables and the data (5). Viewing the mesh as a periodic portion of the Auslander–Reiten (AR) quiver in the derived category of representation of type  $A$  quivers, we obtain the scattering amplitudes directly. This may be related to the geometric constructions through [17, 18]. Before proceeding to the categorical framework let us make the above constructions concrete through some illustrations studied previously in the literature.

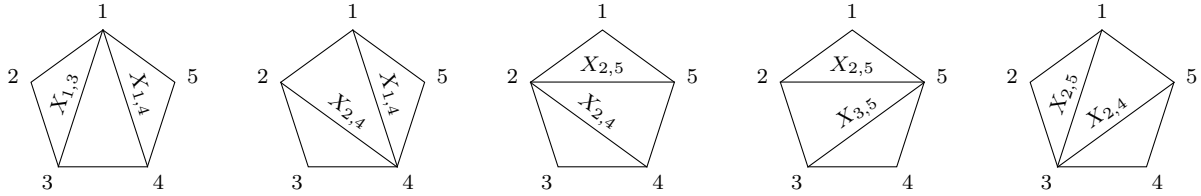


Figure 3: Triangulations of a pentagon in  $\phi^3$  theory ( $m = 1$ )

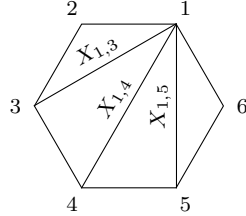


Figure 4: A triangulation of a hexagon in  $\phi^3$  theory ( $m = 1$ )

**Example 1** (Cubic theory). This case, with  $m = 1$ , thus  $N = n + 2$ , by (2), has been dealt with earlier [15]. Let us first consider the  $N = 5$  case, with  $n = 3$ . There are five planar diagrams obtained as duals of five non-identical triangulations of a pentagon shown in Fig 3. For example, the third triangulation corresponds to the Feynman diagram

$$\begin{array}{c}
 2 \quad \quad \quad 1 \\
 \diagdown \quad \quad \diagup \\
 \quad X_{2,4} \quad \quad \quad \\
 \diagup \quad \quad \diagdown \\
 3 \quad \quad \quad 5 \\
 \quad \quad \quad | \\
 \quad \quad \quad 4
 \end{array}
 \quad (23)$$

where we used (16) to write  $s_{23} = X_{2,4}$  and  $s_{15} = s_{234} = X_{2,5}$ . The scattering amplitude is a sum of five terms, one for each Feynman diagram. In terms of the diagonals of the triangulation of the pentagon, the amplitude reads

$$S_5(\phi^3) = \frac{1}{X_{1,3}X_{1,4}} + \frac{1}{X_{1,4}X_{2,4}} + \frac{1}{X_{2,4}X_{2,5}} + \frac{1}{X_{2,5}X_{3,5}} + \frac{1}{X_{3,5}X_{1,3}}, \quad (24)$$

the third term coming from (23). The mesh diagram

$$\begin{array}{ccccc}
 & 1,4 & & 2,5 & & 1,3 & \\
 & \nearrow & \searrow & \nearrow & \searrow & \nearrow & \searrow \\
 1,3 & & 2,4 & & 3,5 & & 1,4
 \end{array}
 \quad (25)$$

is obtained from (18) after omitting the null entries. Let us stress that the mesh consists in all the diagonals that appear in all the triangulations corresponding to the planar diagrams. The terms in (24) are obtained directly by identifying the mesh as the cluster category of the AR quiver of an  $A_{N-3} = A_2$  quiver [15]. Each term contains the projectives of hearts of intermediate  $t$ -structures of the derived category of representations of  $A_2$  restricted to the cluster category. Similarly, for  $N = 6$ , the three diagonals of all the



triangulations of a hexagon, one of which is shown in Fig. 4, appear in the scattering amplitude, given by

$$\begin{aligned}
S_6(\phi^3) = & \frac{1}{X_{1,3}X_{1,4}X_{1,5}} + \frac{1}{X_{1,5}X_{2,4}X_{2,5}} + \frac{1}{X_{1,5}X_{1,4}X_{2,4}} + \frac{1}{X_{2,4}X_{2,5}X_{2,6}} + \frac{1}{X_{2,5}X_{2,6}X_{3,5}} \\
& + \frac{1}{X_{2,6}X_{3,5}X_{3,6}} + \frac{1}{X_{2,6}X_{3,6}X_{4,6}} + \frac{1}{X_{1,5}X_{2,5}X_{3,5}} + \frac{1}{X_{1,3}X_{1,4}X_{4,6}} + \frac{1}{X_{1,3}X_{1,5}X_{3,5}} \\
& + \frac{1}{X_{1,4}X_{2,4}X_{4,6}} + \frac{1}{X_{1,3}X_{3,6}X_{4,6}} + \frac{1}{X_{2,4}X_{2,6}X_{4,6}} + \frac{1}{X_{1,3}X_{3,5}X_{3,6}}. \quad (26)
\end{aligned}$$

The mesh diagram in this case is

$$\begin{array}{cccccc}
& & 1,5 & & 2,6 & & 1,3 & & \\
& & \nearrow & & \searrow & & \nearrow & & \searrow \\
& 1,4 & & 2,5 & & 3,6 & & 1,4 & \\
& \nearrow & & \searrow & & \nearrow & & \searrow & \\
1,3 & & 2,4 & & 3,5 & & 4,6 & & 1,5
\end{array} \quad (27)$$

There are fourteen Feynman diagrams contributing to the scattering amplitude, which is again written directly in terms of the projectives from the mesh (27) identified as the cluster category of an  $A_{N-3} = A_3$  quiver [15].

In this article we present a generalization of this approach to other, more general, potentials. This brings in the paraphernalia of higher cluster categories. In this section we obtain the mesh diagrams in a few more general examples, postponing the categorical description to section 4.

**Example 2** (Quartic theory). Planar diagrams of  $N$ -particle scattering in a quartic theory, with  $V(\phi) = \lambda_4 \phi^4$ , that is,  $m = 2$ , correspond to quadrangulations of  $N$ -gons, shown in Fig. 5 for  $N = 8, 10$ . The quadrangulations are classified into Stokes polytopes and

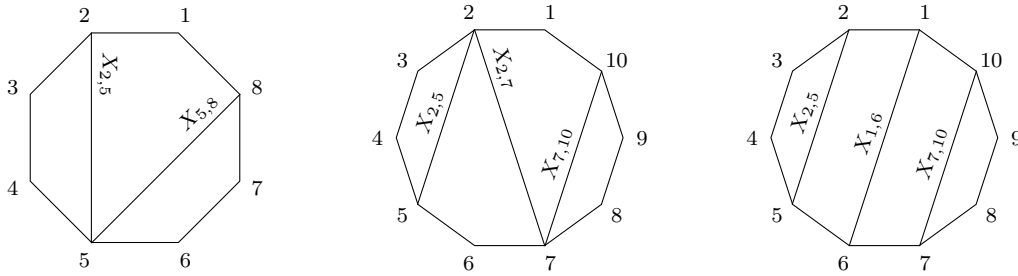


Figure 5: Some quadrangulations of  $(2n + 2)$ -gons in  $\phi^4$  theory ( $m = 2$ )

the scattering amplitude can be obtained considering all such quadrangulations [6, 9]. For  $N = 8$  and  $n = 3$ , corresponding to three quartic vertices in a planar diagram, the partition is  $\Lambda = (2, 2, 2)$  yielding the mesh

$$\begin{array}{cccccc}
& 1,6 & 3,8 & 2,5 & 4,7 & 1,6 \\
& \nearrow & \searrow & \nearrow & \searrow & \nearrow \\
1,4 & & 3,6 & & 5,8 & & 2,7 & & 1,4
\end{array}, \quad (28)$$

while for  $N = 10$  the mesh is

$$\begin{array}{cccccccc}
 & & 1,8 & 3,10 & 2,5 & 4,7 & 6,9 & 1,8 \\
 & \nearrow & \searrow & \nearrow & \searrow & \nearrow & \searrow & \nearrow \\
 & 1,6 & & 3,8 & & 5,10 & & 2,7 & & 4,9 & & 1,6 \\
 & \nearrow & \searrow & \nearrow & \searrow & \nearrow & \searrow & \nearrow & \searrow & \nearrow & \searrow & \nearrow \\
 1,4 & & 3,6 & & 5,8 & & 7,10 & & 2,9 & & 1,4
 \end{array}, \tag{29}$$

with  $\Lambda = (2, 2, 2, 2)$ . As mentioned earlier, these are obtained from (18), starting with the first slice, selecting entries in steps of 2, starting from  $X_{1,2}$ . For example, with  $N = 10$ , the entries selected from the first slice are

$$X_{1,2} - X_{1,4} - X_{1,6} - X_{1,8} - X_{1,10}.$$

The slices are then chosen in steps of 2, selecting the ones starting with the null entries  $X_{3,4}$ ,  $X_{5,6}$ ,  $X_{7,8}$  and  $X_{9,10}$ . After this the first slice is repeated. Omitting the null entries now yields the mesh (29). In the categorical approach the amplitude is obtained by writing down the mesh directly.

Planar diagrams contributing to the scattering amplitude in a theory with a generic polynomial potential (1) are dual to mixed angulations of  $N$ -gons. Let us discuss an example. More general examples will be discussed in section 4.

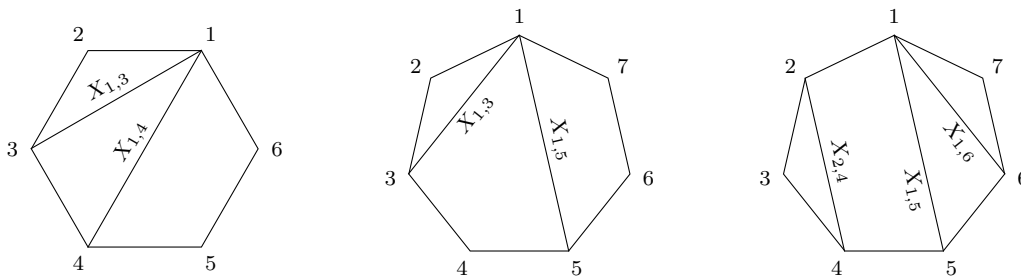
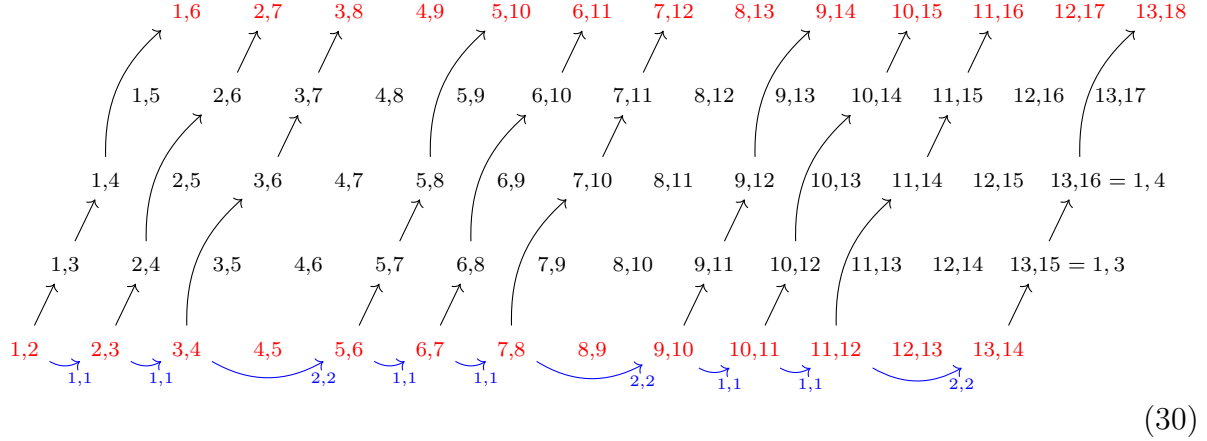


Figure 6: Mixed angulations for  $N = 6$  and  $N = 7$  in  $V(\phi) = \lambda_3\phi^3 + \lambda_4\phi^4$  theory

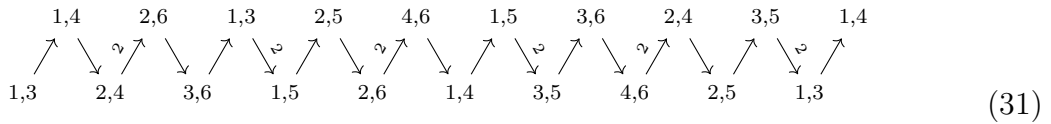
**Example 3** ((3, 4) theory). Let us consider the interaction potential  $V(\phi) = \lambda_3\phi^3 + \lambda_4\phi^4$ , so that  $(m_1, m_2) = (1, 2)$ . The angulations involve triangles and quadrangles. For example,  $(n_1, n_2) = (2, 1)$  for  $N = 6$ , so that the angulations have two triangles and one quadrangle [11], as in the first diagram of Fig. 6. For  $N = 7$  two cases arise from the solutions of (5), namely,  $(n_1, n_2) = (1, 2)$ , corresponding to one triangle and two quadrangles and  $(n_1, n_2) = (3, 1)$ , corresponding to three triangles and one quadrangle, as demonstrated in the second and third diagrams in Fig. 6, respectively.

Let us describe the derivation of the mesh for  $N = 6$  with the partition  $\Lambda = (1, 1, 2)$  in detail. This is sufficiently general to cover all the aspects of the construction. The cases studied earlier are simpler special cases. As described before, the first slice commences with  $X_{1,2}$  and the second index is incremented successively by  $\Lambda$ , yielding  $X_{1,2} \rightarrow X_{1,3} \rightarrow X_{1,4} \rightarrow X_{1,6}$ , as shown in (30). In the bottom row, again starting with  $X_{1,2}$ ,

both the indices are incremented by equal amounts by entries of  $\Lambda$ , as indicated by the blue arrows in (30), proceeding till the first slice is repeated. Let us remark that for odd values of  $N$  the slice is repeated with same direction of arrows among the nodes, but sense reversed, from top to bottom, instead of bottom to top, which is the order in the first slice.



Discarding the top and bottom rows yields the mesh



Let us emphasize that the blue arrows, discarded along with the bottom row, are not part of the mesh diagram. We have thus obtained the mesh diagram in terms of the planar variables. While these may be associated to angulations and thence to the dual planar diagrams, the present construction is algebraic, without alluding to the angulations. The mesh diagrams are identical to certain orbit categories within the bounded derived category of representations of quivers of  $A$ -type up to further identifications. Let us now discuss various notions leading to this identification.

### 3 Derived categories and quiver representations

We briefly recollect various notions pertinent to the categorical approach. In order to keep the article more-or-less self-contained we include some pedagogical material as well [19–24].

#### 3.1 Quiver representations

A *quiver*  $Q$  is a directed graph consisting of a set of directed edges between a set of vertices. In the context of this article, we work exclusively with quivers of type  $A$ , which are directed graphs whose underlying undirected graphs are Dynkin diagrams of type  $A$ . Moreover, we choose the following linear orientation for a quiver of type  $A_n$

$$\bullet^1 \longrightarrow \bullet^2 \longrightarrow \dots \longrightarrow \bullet^n \tag{32}$$

	<i>type A<sub>2</sub></i>	<i>type A<sub>3</sub></i>	
<i>quiver</i>	$\bullet^1 \longrightarrow \bullet^2$	$\bullet^1 \longrightarrow \bullet^2 \longrightarrow \bullet^3$	
<i>indecomposable representations</i>	$1 := \mathbf{C} \longrightarrow 0$ $2 := 0 \longrightarrow \mathbf{C}$ $\frac{1}{2} := \mathbf{C} \xrightarrow{\text{id}} \mathbf{C}$	$1 := \mathbf{C} \longrightarrow 0 \longrightarrow 0$ $2 := 0 \longrightarrow \mathbf{C} \longrightarrow 0$ $3 := 0 \longrightarrow 0 \longrightarrow \mathbf{C}$	$\frac{1}{2} := \mathbf{C} \xrightarrow{\text{id}} \mathbf{C} \longrightarrow 0$ $\frac{2}{3} := 0 \longrightarrow \mathbf{C} \xrightarrow{\text{id}} \mathbf{C}$ $\frac{1}{2}_3 := \mathbf{C} \xrightarrow{\text{id}} \mathbf{C} \xrightarrow{\text{id}} \mathbf{C}$

Figure 7: The indecomposable representations of the quivers of type  $A_2$  and type  $A_3$

where we label the vertices by  $1, \dots, n$ .

A *representation* of a quiver  $Q$  is given by assigning a finite-dimensional  $\mathbf{C}$ -vector space  $V_i$  to each vertex  $\bullet^i$  and a linear map  $f_{ij}: V_i \rightarrow V_j$  to each edge  $\bullet^i \rightarrow \bullet^j$ . Representations of a quiver  $Q$  form an Abelian category denoted  $\text{rep } Q$  with morphisms  $\phi: V \rightarrow W$  between two representations  $V = ((V_i)_i, (f_{ij})_{i,j})$  and  $W = ((W_i)_i, (g_{ij})_{i,j})$  given by commutative diagrams

$$\begin{array}{ccc}
 V_i & \xrightarrow{f_{ij}} & V_j \\
 \downarrow & & \downarrow \\
 W_i & \xrightarrow{g_{ij}} & W_j
 \end{array}$$

This category turns out to be Krull–Schmidt, i.e. every representation can be written uniquely (up to ordering of the direct summands) as the direct sum of indecomposable representations. In general, an explicit description of  $\text{rep } Q$  can be quite complicated. However, for quivers of type  $A$  there are only finitely many indecomposable representations up to isomorphism which for the linearly oriented quiver (32) are all of the form

$$\begin{array}{c} i \\ \vdots \\ j \end{array} := 0 \longrightarrow \dots \longrightarrow 0 \longrightarrow \mathbf{C} \xrightarrow{\text{id}} \dots \xrightarrow{\text{id}} \mathbf{C} \longrightarrow 0 \longrightarrow \dots \longrightarrow 0.$$

Fig. 7 lists all the indecomposable representations for quivers of type  $A_2$  and type  $A_3$ .

Since  $\text{rep } Q$  is a *hereditary* category — i.e.  $\text{Ext}_{\text{rep } Q}^i(V, W) = 0$  for all  $i \geq 2$  and all representations  $V, W$  in  $\text{rep } Q$  — the classification of indecomposable representations together with the description of the short exact sequences between them completely characterizes the Abelian category  $\text{rep } Q$ .

The indecomposable representations for  $\text{rep } Q$  can be woven into a mesh indicating the so-called *almost-split exact* sequences, which are building blocks of the short exact sequences in  $\text{rep } Q$ . This mesh is called the Auslander–Reiten quiver of the Abelian category  $\text{rep } Q$ . In case of the quiver (32) of type  $A_n$ , the Auslander–Reiten quiver of



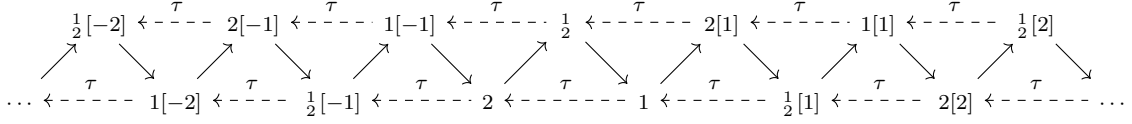


Figure 8: The Auslander–Reiten quiver of the derived category of the  $A_2$  quiver

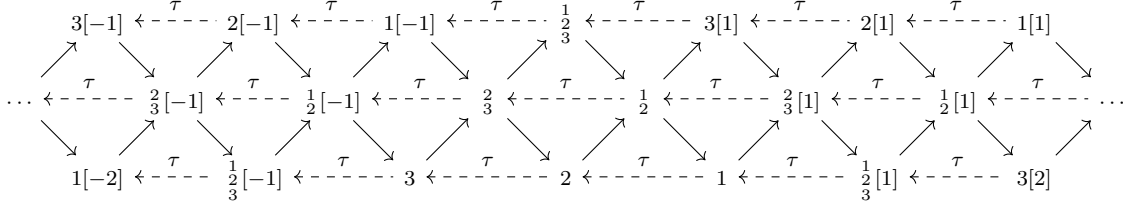


Figure 9: The Auslander–Reiten quiver of the derived category of the  $A_3$  quiver

as

$$\begin{array}{ccc}
 & C & \\
 [1] \swarrow & & \nwarrow \\
 A & \longrightarrow & B
 \end{array}$$

More generally, the triangulated structure of  $D(\mathcal{A})$  allows one to look at the cone of a morphism  $A^\bullet \rightarrow B^\bullet$  between two arbitrary complexes, not necessarily concentrated in degree 0, which may be completed to a so-called distinguished triangle  $A^\bullet \rightarrow B^\bullet \rightarrow C^\bullet \rightarrow A^\bullet[1]$  (see e.g. [23] for more details).

### 3.2.1 Derived categories of quiver representations

Since  $\text{rep } Q$  is hereditary, any complex in the derived category  $D(\text{rep } Q)$  is quasi-isomorphic to a complex with all differentials  $d^i$  being the zero map. The indecomposable objects of  $D(\text{rep } Q)$  are thus of the form  $V[k]$  where  $V$  is an indecomposable representation in  $\text{rep } Q$  viewed as a complex concentrated in degree  $-k$ .

As in the case of the Abelian category  $\text{rep } Q$ , the derived category is completely characterized by its Auslander–Reiten quiver. The derived category has another natural automorphism  $\tau: D(\text{rep } Q) \rightarrow D(\text{rep } Q)$ , called the *Auslander–Reiten translation* which is characterized by  $\text{Hom}(V, \tau(V)[1]) \neq 0$ , leading to the existence of a triangle  $\tau(V) \rightarrow W \rightarrow V \rightarrow \tau(V)[1]$ . Figs. 8 and 9 exhibit the Auslander–Reiten quivers of the derived categories of the  $A_2$  and  $A_3$  quivers, respectively. Let us point out that the Auslander–Reiten quiver of the Abelian categories  $\text{rep } A_2$  and  $\text{rep } A_3$  (33) appears in the middle of the diagram, as complexes concentrated in degree 0.

### 3.3 $t$ -structures

The formalism of  $t$ -structures is a means to vivisect a triangulated category. A  $t$ -structure on a triangulated category  $\mathcal{D}$  is a pair  $(\mathcal{D}^{\leq 0}, \mathcal{D}^{\geq 0})$  of strictly full subcategories, satisfying the following conditions.

1.  $\mathcal{D}^{\leq 0}[1] \subset \mathcal{D}^{\leq 0}$  and  $\mathcal{D}^{\geq 0} \subset \mathcal{D}^{\geq 0}[1]$
2.  $\mathrm{Hom}_{\mathcal{D}}(\mathcal{D}^{\leq 0}, \mathcal{D}^{\geq 0}[-1]) = 0$
3. For each object  $K$  of  $\mathcal{D}$ , there exists a distinguished triangle  $X \rightarrow K \rightarrow Y[-1] \rightarrow X[1]$  with  $X \in \mathcal{D}^{\leq 0}$  and  $Y \in \mathcal{D}^{\geq 0}$ .

Further, a  $t$ -structure is called *bounded* if each  $K$  in  $\mathcal{D}$  is contained in  $\mathcal{D}^{\leq 0}[m] \cap \mathcal{D}^{\geq 0}[n]$  for some integers  $m$  and  $n$  and any bounded  $t$ -structure is determined by its *heart*  $\mathcal{D}^{\leq 0} \cap \mathcal{D}^{\geq 0}$ , which is always an Abelian category. All  $t$ -structures considered in this article are bounded.

Finally, an object  $P \in \mathcal{D}$  is called a *projective* of the heart if for all  $M \in \mathcal{H}$  and all  $k \neq 0$  one has  $\mathrm{Hom}_{\mathcal{D}}(P, M[k]) = 0$ . For type  $A$  quivers the dimension of the Hom space between indecomposable objects can be read off the AR quiver [20, §3.1.4].

#### 3.3.1 Standard $t$ -structure

Let  $\mathcal{D} = D(\mathcal{A})$  be the derived category of an Abelian category  $\mathcal{A}$  with its usual triangulated structure. Let  $\mathcal{D}^{\geq n}$  denote the full subcategory of  $\mathcal{D}$  formed by complexes  $A^\bullet$  with cohomology only beyond  $n$ , that is,  $H^i(A^\bullet) = 0$  for  $i < n$ . Similarly, let  $\mathcal{D}^{\leq n}$  denote the full subcategory of  $D(\mathcal{A})$  of complexes  $A^\bullet$  with cohomology only below  $n$ , that is  $H^i(A^\bullet) = 0$  for  $i > n$ .

Then  $(\mathcal{D}^{\leq 0}, \mathcal{D}^{\geq 0})$  is called the *standard  $t$ -structure* and its heart  $\mathcal{D}^{\leq 0} \cap \mathcal{D}^{\geq 0} \simeq \mathcal{A}$  recovers the original Abelian category viewed as complexes concentrated in degree 0.

#### 3.3.2 Intermediate $t$ -structures

Let  $(\mathcal{D}^{\leq 0}, \mathcal{D}^{\geq 0})$  denote the standard  $t$ -structure on  $\mathcal{D} = D(\mathcal{A})$  with heart  $\mathcal{D}^{\leq 0} \cap \mathcal{D}^{\geq 0} \simeq \mathcal{A}$ . For any positive integer  $m$ , an  $m$ -*intermediate  $t$ -structure* is any  $t$ -structure  $(\mathcal{D}^{\leq 0}, \mathcal{D}^{\geq 0})$  satisfying  $\mathcal{D}^{\leq 0} \subset \mathcal{D}^{\leq 0} \subset \mathcal{D}^{\leq 0}[m]$  [25], and a 1-intermediate  $t$ -structure is usually simply called *intermediate*. The heart of this new  $t$ -structure is again an Abelian category which may or may not be equivalent to  $\mathcal{A}$ .

Figs. 10 and 11 give an illustration of the 1- and 2-intermediate  $t$ -structures on  $\mathcal{D}_{A_2} = D^b(\mathrm{rep} A_2)$ . Each diagram is a picture of the Auslander–Reiten quiver of the derived category  $\mathcal{D}_{A_2}$  described in Fig. 8. The vertices correspond to indecomposable objects, with the filled vertices corresponding to the complexes concentrated in degree 0, i.e. the indecomposable objects in the heart of the standard  $t$ -structure. Each diagram illustrates some  $t$ -structure  $(\mathcal{D}_{A_2}^{\leq 0}, \mathcal{D}_{A_2}^{\geq 0})$ , the blue part corresponds to  $\mathcal{D}_{A_2}^{\leq 0}$  and the red part to  $\mathcal{D}_{A_2}^{\geq 0}[-1]$  of the  $t$ -structure. The vertices in the shaded part correspond to the indecomposable objects in the heart of the  $t$ -structure, which is given by  $\mathcal{D}_{A_2}^{\leq 0} \cap \mathcal{D}_{A_2}^{\geq 0}$ . Diagrammatically, the heart is obtained as the intersection of the blue part and the shift (given by glide reflection to the right) of the red part.

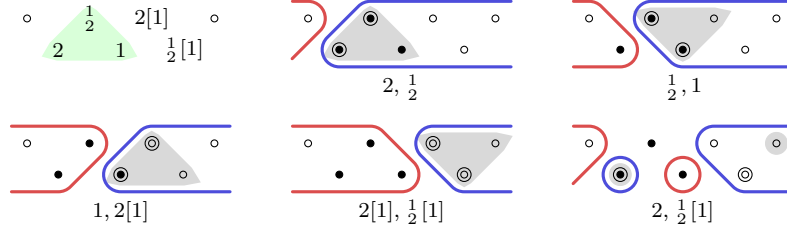


Figure 10: The five intermediate  $t$ -structures of  $\mathcal{D}_{A_2}$ , their hearts (shaded) and projective objects (circled vertices). The standard heart is marked in Green.

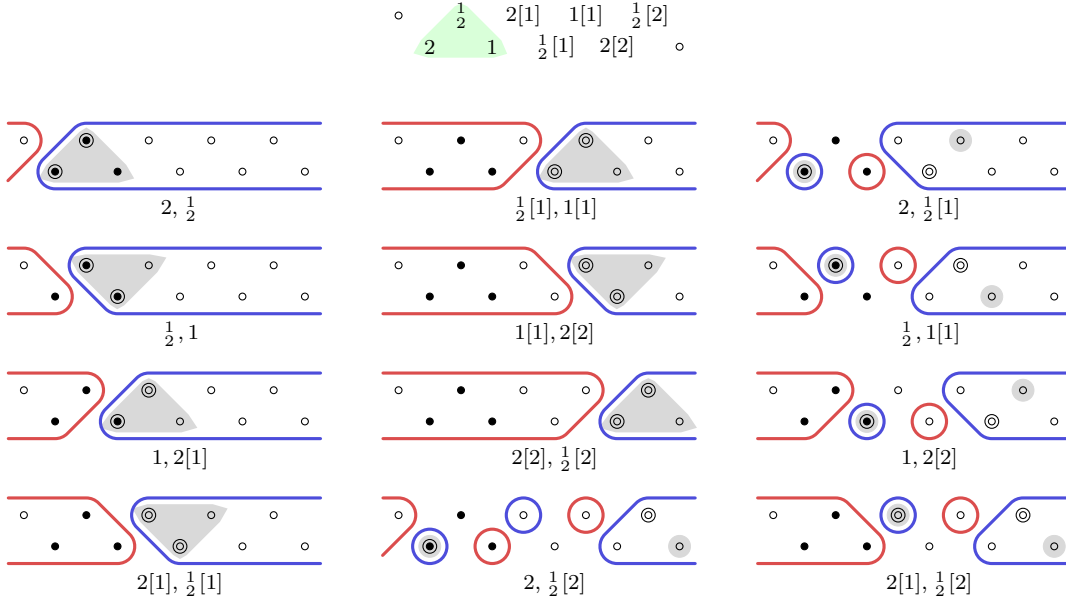


Figure 11: The twelve 2-intermediate  $t$ -structures of  $\mathcal{D}_{A_2}$ , their hearts (shaded), projective objects (circled vertices). The standard heart is marked in Green.

As we show in this article, each  $m$ -intermediate  $t$ -structure corresponds to a term in the scattering amplitude in a  $\phi^{m+2}$  theory.

### 3.4 Orbit categories

Given an additive category  $\mathcal{D}$  — in particular the derived category of quiver representations — together with an automorphism  $g: \mathcal{D} \rightarrow \mathcal{D}$ , an *orbit category*  $\mathcal{D}/g$  (also denoted  $\mathcal{D}/g^{\mathbf{Z}}$ ) is defined by taking the same objects as  $\mathcal{D}$  and taking morphisms from  $X$  to  $Y$  to be in bijection with

$$\bigoplus_{n \in \mathbf{Z}} \text{Hom}_{\mathcal{D}}(X, g^n(Y)),$$

where  $\mathbf{Z}$  denotes the set of integers. Two important examples of such automorphisms are

1. the  $N$ -th power  $[1]^N = [N]: \mathcal{D} \rightarrow \mathcal{D}$  of the shift functor



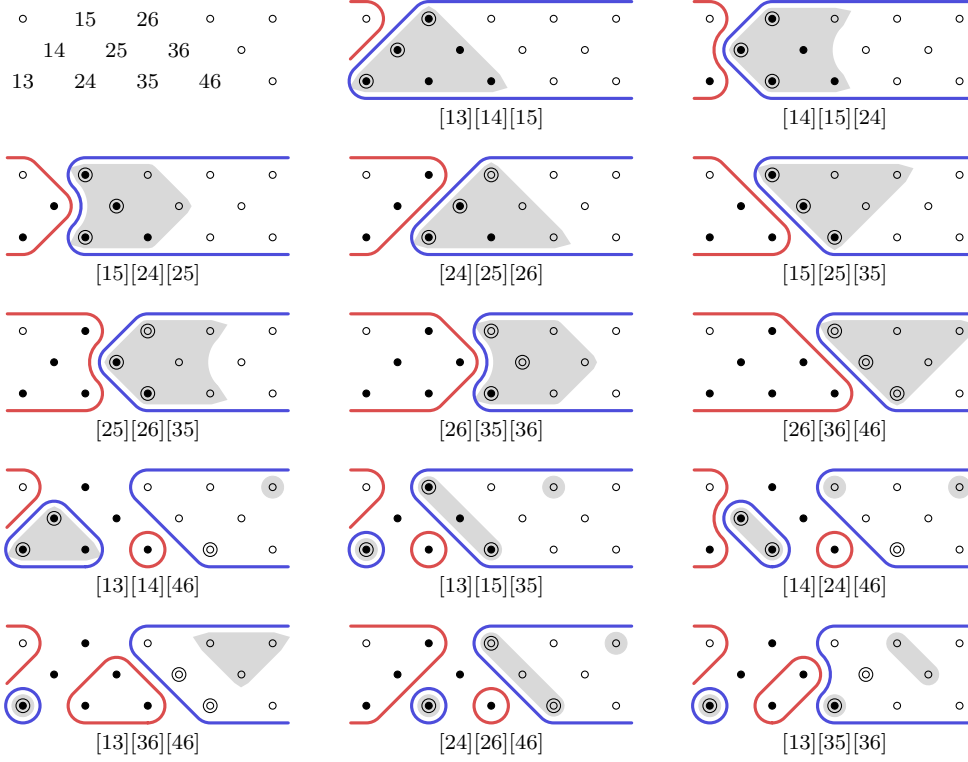


Figure 12: The 14 intermediate  $t$ -structures of  $\mathcal{D}_{A_3}$  obtained by tilting from the standard heart (filled vertices), their hearts (shaded), projective objects (circled vertices) and their contribution to the scattering amplitude

2. the  $m$ -cluster automorphism  $F^m = \tau^{-1} \circ [m]: \mathcal{D} \rightarrow \mathcal{D}$ , where  $\tau$  is the Auslander–Reiten translation.

The corresponding orbit categories are

1. the  $N$ -periodic derived category  $\mathcal{P}^N = \mathcal{D}/[N]$
2. the  $m$ -cluster category  $\mathcal{C}^m = \mathcal{D}/(\tau^{-1} \circ [m])$

which both naturally inherit a triangulated structure from  $\mathcal{D}$  [26, 27].

Thus, in an  $m$ -cluster category the AR translation and the shift functors are related by

$$\tau^{-1} \circ [m] \simeq \text{id}. \quad (35)$$

The AR quiver of these categories appear as the mesh diagrams for potentials of the form  $V(\phi) = \phi^{m+2}$ . In an  $N$ -periodic category, on the other hand,

$$[1]^N \simeq \text{id}. \quad (36)$$

The quotient that appears for a generic polynomial is a variant of the periodic category. In addition to the identification (36), the corresponding mesh diagram entails identification of intervening entries. We refer to it suggestively as a *pseudo-periodic category*, although we

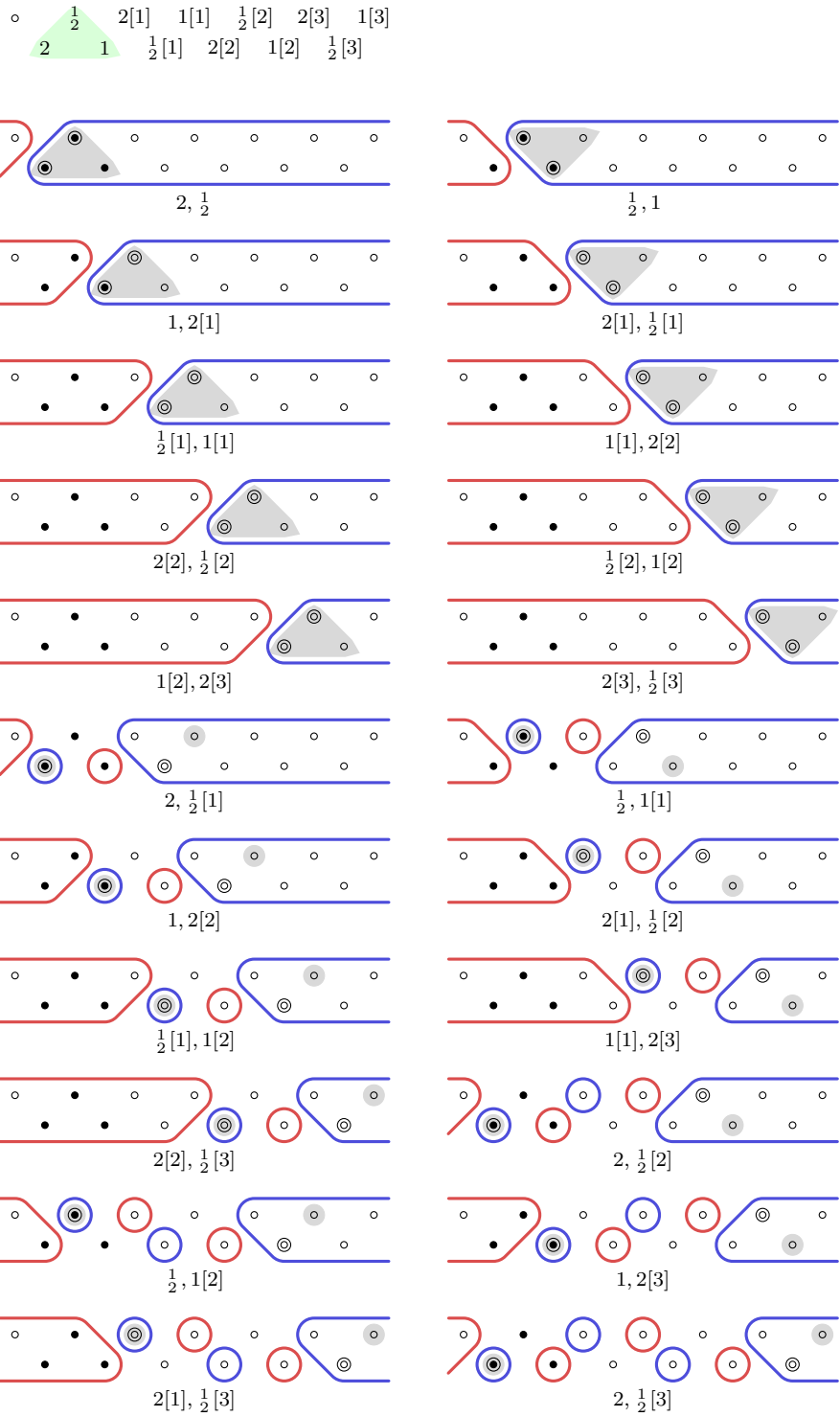


Figure 13: The 22 3-intermediate  $t$ -structures of  $\mathcal{D}_{A_2}$ , their hearts (shaded), projective objects (circled vertices). The standard heart is marked in green.

have not studied its categorical structure here. As the scattering amplitude for polynomial potentials can be categorified via certain partial cluster tilting objects in a cluster category, the unknown structure of the pseudo-periodic category, however, does not undermine the rigour of the categorification we show.

Let us point out some features of this, arising from the combinatorics of planar diagrams. First, we have, for the AR quiver of an  $A_{n-1}$  quiver, a relation between the shift functor and the AR translation,

$$[1]^2 \simeq \tau^{-n}, \tag{37}$$

by the very definition of the functors. Using (5) and (6) arising in the combinatorics of Feynman diagrams in (36) and (37) we obtain

$$\tau^{-\sum_i n_i} [\sum_i m_i n_i] \simeq \text{id}. \tag{38}$$

Since the AR translation  $\tau$  and the shift  $[1]$  commute, this can be written as

$$\prod_i (F^{m_i})^{n_i} = 1, \tag{39}$$

where the product means successive composition of the functors  $(F^{m_i})^{n_i}$ . However, the pseudo-periodic category has further identifications besides the periodic structure, which are not realized by the identifications given by the cyclic group generated by a single automorphism. In the case of a single term in the potential,  $V(\phi) = \phi^{m+2}$ , (39) reduces to

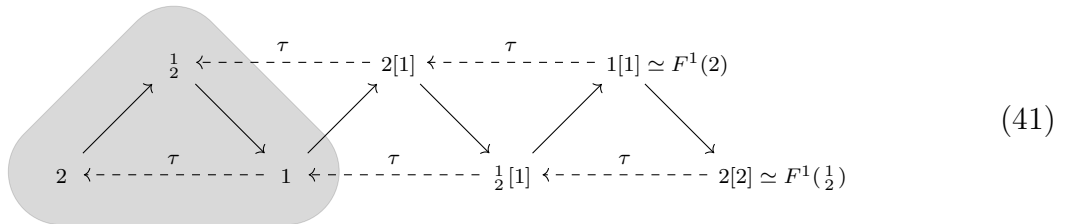
$$(F^m)^n \simeq \text{id}, \tag{40}$$

which is solved by (35).

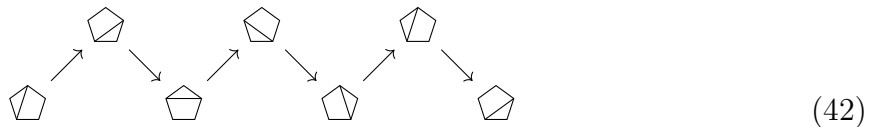
Let us now list some examples of cluster categories of  $A_{n-1}$  quivers to be used to derive the scattering amplitudes. We denote the  $m$ -cluster category of an  $A_n$  quiver by  $\mathcal{C}_{A_n}^m = \mathcal{D}_{A_n}/(\tau^{-1} \circ [m])$ . For  $m = 1$ , it is called a cluster category and the superscript is suppressed. The  $N$ -periodic category of an  $A_n$  quiver is denoted  $\mathcal{P}_{A_n}^N = \mathcal{D}_{A_n}/[N]$ .

### 3.4.1 Cluster categories

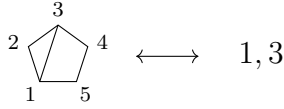
The cluster category  $\mathcal{C}_{A_2}$  is obtained by setting  $F^1 = \tau^{-1} \circ [1] \simeq \text{id}$ , namely,



where  $1[1]$  is identified with  $2$  and  $2[2]$  with  $\frac{1}{2}$ . This diagram can be written geometrically by associating to each indecomposable object a diagonal in a triangulation of a pentagon, i.e.

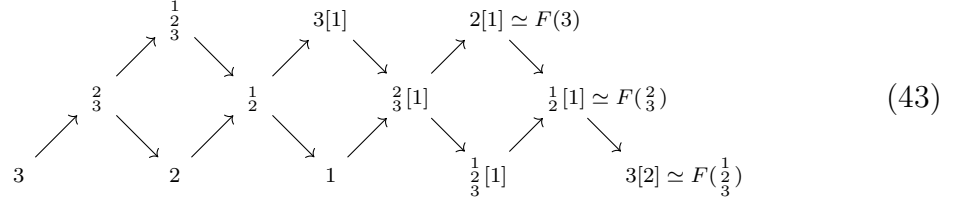


Labelling each vertex with a positive natural number and each diagonal by the two vertices it connects, e.g.

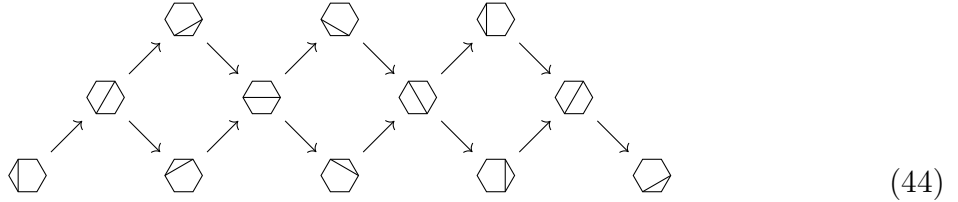


the mesh diagram (25) is recovered.

The cluster category  $\mathcal{C}_{A_3}$  is similarly given by



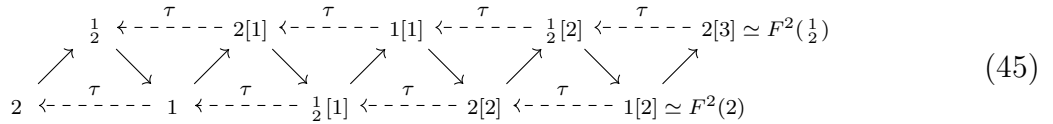
and can likewise be written geometrically as



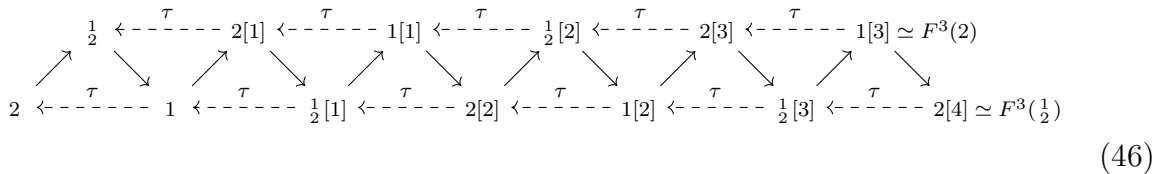
leading to the mesh diagram (27).

### 3.4.2 Higher cluster categories

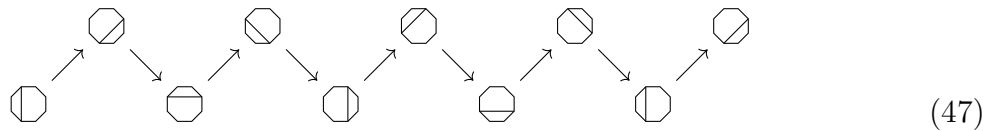
The 2-cluster category  $\mathcal{C}_{A_2}^2$  is obtained by identifying  $F^2 = \tau^{-1} \circ [2] \simeq \text{id}$ , leading to



The 3-cluster category  $\mathcal{C}_{A_2}^3$  with  $F^3 = \tau^{-1} \circ [3] \simeq \text{id}$  is given by

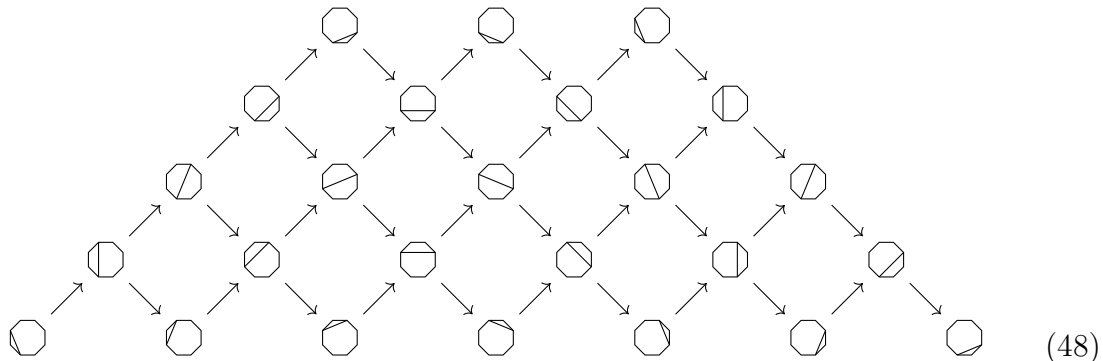


The geometric analogue of the higher cluster categories are diagonals of an  $N$ -gon that form part of an  $(m+2)$ -angulation, where  $N = nm+2$ . Here  $n$  corresponds to the number of  $(m+2)$ -gons in an  $(m+2)$ -angulation [17]. For example, considering a quadrangulation ( $m = 2$ ) of an octagon ( $N = 8$ ), we can write (45) as



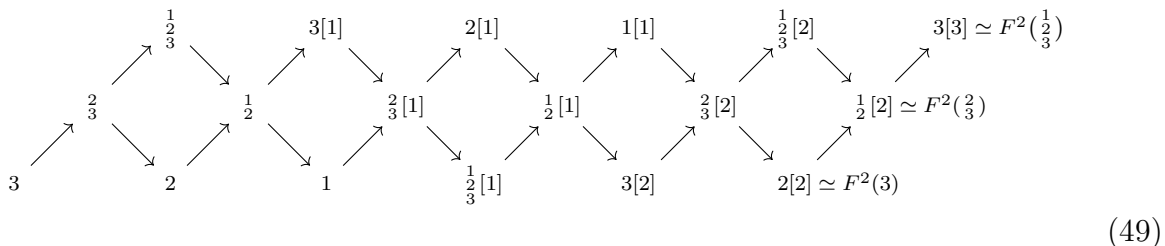
where the identical diagrams on the left and right are identified.

As discussed in section 2, the diagonals of an  $(m + 2)$ -angulation are but a proper subset of those of triangulations of the same  $N$ -gon, obtained by omitting some of the diagonals of the latter. Concretely, the diagonals in (47) appear in the cluster category  $\mathcal{C}_{A_5}$  of an  $A_5$  quiver, describing the triangulations of an octagon. The 2-cluster category  $\mathcal{C}_{A_2}^2$  can thus be viewed as a full extension-closed subcategory of  $\mathcal{C}_{A_5}$  given by the objects on the second and fourth rows of the following diagram



depicting the cluster category  $\mathcal{C}_{A_5}$ . Let us note that on the level of the representations, the objects of  $\mathcal{C}_{A_2}^2$  viewed as a subcategory of  $\mathcal{C}_{A_5}$  correspond precisely to the even-dimensional representations of the  $A_5$  quiver.

The 2-cluster category of  $A_3$  is given by



which can be written as diagonals forming part of a quadrangulation of a decagon and  $\mathcal{C}_{A_3}^2$  can be viewed as a full extension-closed subcategory of  $\mathcal{C}_{A_7}$ .

### 3.4.3 Cluster tilting objects

For  $N = mn + 2$ , the  $m$ -intermediate  $t$ -structures discussed in §3.3.2 are in one-to-one correspondence to  $m$ -cluster tilting objects in  $\mathcal{C}_{A_{n-1}}^m$  and the diagonals of  $m$ -angulations of an  $N$ -gon as in (47) [18, 25, 28]. Concretely, the direct sum of the projectives of the heart of an  $m$ -intermediate  $t$ -structure is an  $m$ -cluster tilting object for  $\mathcal{C}_{A_{n-1}}^m$  and every  $m$ -cluster tilting object arises in this way.

Viewing the  $m$ -cluster category as an extension-closed subcategory of the cluster category  $\mathcal{C}_{A_{N-3}}$ , the  $m$ -cluster tilting objects of  $\mathcal{C}_{A_{n-1}}^m$  correspond to partial cluster tilting objects of  $\mathcal{C}_{A_{N-3}}$ . This point of view is also useful in categorifying the scattering amplitudes for general polynomial potentials.

### 3.4.4 Periodic triangulated categories

The pseudo-periodic categories that appear in the computation of scattering amplitudes are modelled after the periodic categories. Let us list some periodic categories to be used in the examples later on. The 6-periodic category  $\mathcal{P}_{A_2}^6$  of the  $A_2$  quiver is

$$\begin{array}{cccccccccccc}
 & \frac{1}{2} & & 2[1] & & 1[1] & & \frac{1}{2}[2] & & 2[3] & & 1[3] & & \frac{1}{2}[4] & & 2[5] & & 1[5] & & \frac{1}{2}[6] = \frac{1}{2} \\
 & \nearrow & \searrow & \nearrow & \searrow & \nearrow & \searrow & \nearrow & \searrow & \nearrow & \searrow & \nearrow & \searrow & \nearrow & \searrow & \nearrow & \searrow & \nearrow & \searrow & \nearrow \\
 2 & \xleftarrow{\tau} & 1 & & \frac{1}{2}[1] & & 2[2] & & 1[2] & & \frac{1}{2}[3] & & 2[4] & & 1[4] & & \frac{1}{2}[5] & & 2[6] = 2
 \end{array} \tag{50}$$

The 7-periodic category  $\mathcal{P}_{A_2}^7$  of the  $A_2$  quiver is

$$\begin{array}{cccccccccccc}
 & \frac{1}{2} & & 2[1] & & 1[1] & & \frac{1}{2}[2] & & 2[3] & & 1[3] & & \frac{1}{2}[4] & & 2[5] & & 1[5] & & \frac{1}{2}[6] & & 2[7] = 2 \\
 & \nearrow & \searrow & \nearrow & \searrow & \nearrow & \searrow & \nearrow & \searrow & \nearrow & \searrow & \nearrow & \searrow & \nearrow & \searrow & \nearrow & \searrow & \nearrow & \searrow & \nearrow & \searrow & \nearrow \\
 2 & \xleftarrow{\tau} & 1 & & \frac{1}{2}[1] & & 2[2] & & 1[2] & & \frac{1}{2}[3] & & 2[4] & & 1[4] & & \frac{1}{2}[5] & & 2[6] & & 1[6] & & \frac{1}{2}[7] = \frac{1}{2}
 \end{array} \tag{51}$$

The 8-periodic category  $\mathcal{P}_{A_2}^8$  of the  $A_2$  quiver is

$$\begin{array}{cccccccccccc}
 & \frac{1}{2} & & 2[1] & & 1[1] & & \frac{1}{2}[2] & & 2[3] & & 1[3] & & \frac{1}{2}[4] & & 2[5] & & 1[5] & & \frac{1}{2}[6] & & 2[7] & & 1[7] & & \frac{1}{2}[8] = \frac{1}{2} \\
 & \nearrow & \searrow & \nearrow & \searrow & \nearrow & \searrow & \nearrow & \searrow & \nearrow & \searrow & \nearrow & \searrow & \nearrow & \searrow & \nearrow & \searrow & \nearrow & \searrow & \nearrow & \searrow & \nearrow & \searrow & \nearrow & \searrow & \nearrow \\
 2 & \xleftarrow{\tau} & 1 & & \frac{1}{2}[1] & & 2[2] & & 1[2] & & \frac{1}{2}[3] & & 2[4] & & 1[4] & & \frac{1}{2}[5] & & 2[6] & & 1[6] & & \frac{1}{2}[7] & & 2[8] = 2
 \end{array} \tag{52}$$

The category  $\mathcal{P}_{A_3}^7$  is

$$\begin{array}{cccccccccccc}
 & \frac{1}{2} & & 3[1] & & 2[1] & & 1[1] & & \frac{1}{2}[2] & & 3[3] & & 2[3] & & 1[3] & & \frac{1}{2}[4] & & 3[5] & & 2[5] & & 1[5] & & \frac{1}{2}[6] & & 3[7] = 3 \\
 & \nearrow & \searrow & \nearrow & \searrow & \nearrow & \searrow & \nearrow & \searrow & \nearrow & \searrow & \nearrow & \searrow & \nearrow & \searrow & \nearrow & \searrow & \nearrow & \searrow & \nearrow & \searrow & \nearrow & \searrow & \nearrow & \searrow & \nearrow & \searrow & \nearrow \\
 \frac{2}{3} & & \frac{1}{2} & & \frac{2}{3}[1] & & \frac{1}{2}[1] & & \frac{2}{3}[2] & & \frac{1}{2}[2] & & \frac{2}{3}[3] & & \frac{1}{2}[3] & & \frac{2}{3}[4] & & \frac{1}{2}[4] & & \frac{2}{3}[5] & & \frac{1}{2}[5] & & \frac{2}{3}[6] & & \frac{1}{2}[6] & & \frac{2}{3}[7] = \frac{2}{3} \\
 3 & & 2 & & 1 & & \frac{1}{3}[1] & & 3[2] & & 2[2] & & 1[2] & & \frac{1}{3}[3] & & 3[4] & & 2[4] & & 1[4] & & \frac{1}{3}[5] & & 3[6] & & 2[6] & & 1[6] & & \frac{1}{3}[7] = \frac{1}{3}
 \end{array} \tag{53}$$

The category  $\mathcal{P}_{A_3}^{12}$  to be used later is given in (75) in the Appendix.

## 4 Categorical description of scattering amplitudes

In this section we point out the identification of the mesh diagrams obtained from (18) with the cluster and pseudo-periodic categories of  $A$ -type quivers. We then use the intermediate  $t$ -structure for the former and a variant for the latter case to write down the scattering amplitude in terms of projectives of hearts of intermediate  $t$ -structures.

**Example 5** (Cubic theory [15]). Amplitudes of  $N$ -particle scattering in the cubic theory arise from the cluster category of  $A_{n-1}$  quivers. For  $N = 5$  the mesh diagram (25) can be identified as the cluster category  $\mathcal{C}_{A_2}$  in (41). Let us point out that the objects mapped under the automorphism  $F$  are not indicated in the mesh diagram. The planar variables in (25) are in one-to-one correspondence with the representations in (41) and Fig. 10 according to the dictionary

$$2 \longleftrightarrow X_{1,3} \quad (54)$$

$$\frac{1}{2} \longleftrightarrow X_{1,4} \quad (55)$$

$$1 \longleftrightarrow X_{2,4} \quad (56)$$

$$2[1] \longleftrightarrow X_{2,5} \quad (57)$$

$$\frac{1}{2}[1] \longleftrightarrow X_{3,5}, \quad (58)$$

relating representations and diagonals as in (42). Restricting the intermediate  $t$ -structures Fig. 10 to the cluster category and using the correspondence of  $X$ 's and the objects of  $\mathcal{C}_{A_2}$  we find that the amplitude (24) is given term by term in terms of the projectives of the hearts of intermediate  $t$ -structures.

For the  $N = 6$  case, similarly, the mesh diagram (27) is identified with the cluster category  $\mathcal{C}_{A_3}$  in (43). The amplitude (26) is then obtained term by term through the correspondence between  $X$ 's and the representations in the cluster category from the projectives of hearts of the intermediate  $t$ -structures Fig. 12 restricted to  $\mathcal{C}_{A_3}$ .

**Example 6** (Quartic theory). The amplitudes of  $N$ -particle scattering for the quartic theory with  $m = 2$  are obtained from the 2-cluster category  $\mathcal{C}_{A_{n-1}}^2$ . For example, for  $N = 8$ ,  $n = 3$ ,  $\Lambda = (2, 2, 2)$ . The mesh (28) is identified with  $\mathcal{C}_{A_2}^2$  in (45). The 2-intermediate  $t$ -structures are shown in Fig. 11 and Fig. 14 in terms of the representations and the planar variables, respectively. The scattering amplitude is obtained as twelve terms corresponding to the projectives of the hearts in the twelve 2-intermediate  $t$ -structures restricted to  $\mathcal{C}_{A_2}^2$  as

$$\begin{aligned} S_8(\phi^4) = & \frac{1}{X_{1,4}X_{1,6}} + \frac{1}{X_{1,6}X_{3,6}} + \frac{1}{X_{3,6}X_{3,8}} + \frac{1}{X_{3,8}X_{5,8}} \\ & + \frac{1}{X_{5,8}X_{2,5}} + \frac{1}{X_{2,5}X_{2,7}} + \frac{1}{X_{2,7}X_{4,7}} + \frac{1}{X_{4,7}X_{1,4}} \\ & + \frac{1}{X_{1,4}X_{5,8}} + \frac{1}{X_{1,6}X_{2,5}} + \frac{1}{X_{3,6}X_{2,7}} + \frac{1}{X_{3,8}X_{4,7}}. \end{aligned} \quad (59)$$

Similarly, for  $N = 10$ ,  $\Lambda = (2, 2, 2, 2)$  and the mesh (29) matches the 2-cluster category

$\mathcal{C}_{A_3}^2$  given in (49). Using the 2-intermediate  $t$ -structures we obtain the scattering amplitude

$$\begin{aligned}
S_{10}(\phi^4) = & \frac{1}{X_{1,4}X_{1,6}X_{1,8}} + \frac{1}{X_{3,6}X_{3,8}X_{3,10}} + \frac{1}{X_{5,8}X_{5,10}X_{2,5}} + \frac{1}{X_{7,10}X_{2,7}X_{4,7}} + \frac{1}{X_{2,9}X_{4,9}X_{6,9}} \\
& + \frac{1}{X_{1,8}X_{3,8}X_{5,8}} + \frac{1}{X_{3,10}X_{5,10}X_{7,10}} + \frac{1}{X_{2,5}X_{2,7}X_{2,9}} + \frac{1}{X_{4,7}X_{4,9}X_{1,4}} + \frac{1}{X_{6,9}X_{1,6}X_{3,6}} \\
& + \frac{1}{X_{1,8}X_{3,8}X_{3,6}} + \frac{1}{X_{3,10}X_{5,10}X_{5,8}} + \frac{1}{X_{2,5}X_{2,7}X_{7,10}} + \frac{1}{X_{4,7}X_{4,9}X_{2,9}} + \frac{1}{X_{6,9}X_{1,6}X_{1,4}} \\
& + \frac{1}{X_{1,8}X_{1,6}X_{3,6}} + \frac{1}{X_{3,10}X_{3,8}X_{5,8}} + \frac{1}{X_{2,5}X_{5,10}X_{7,10}} + \frac{1}{X_{4,7}X_{2,7}X_{2,9}} + \frac{1}{X_{6,9}X_{4,9}X_{1,4}} \\
& + \frac{1}{X_{1,4}X_{1,6}X_{7,10}} + \frac{1}{X_{3,6}X_{3,8}X_{2,9}} + \frac{1}{X_{5,8}X_{5,10}X_{1,4}} + \frac{1}{X_{7,10}X_{2,7}X_{3,6}} + \frac{1}{X_{2,9}X_{4,9}X_{5,8}} \\
& + \frac{1}{X_{1,4}X_{5,10}X_{7,10}} + \frac{1}{X_{3,6}X_{2,7}X_{2,9}} + \frac{1}{X_{5,8}X_{4,9}X_{1,4}} + \frac{1}{X_{7,10}X_{1,6}X_{3,6}} + \frac{1}{X_{2,9}X_{3,8}X_{5,8}} \\
& + \frac{1}{X_{1,8}X_{3,8}X_{4,7}} + \frac{1}{X_{3,10}X_{5,10}X_{6,9}} + \frac{1}{X_{2,5}X_{2,7}X_{1,8}} + \frac{1}{X_{4,7}X_{4,9}X_{3,10}} + \frac{1}{X_{6,9}X_{1,6}X_{2,5}} \\
& + \frac{1}{X_{1,8}X_{2,7}X_{4,7}} + \frac{1}{X_{3,10}X_{4,9}X_{6,9}} + \frac{1}{X_{2,5}X_{1,6}X_{1,8}} + \frac{1}{X_{4,7}X_{3,8}X_{3,10}} + \frac{1}{X_{6,9}X_{5,10}X_{2,5}} \\
& + \frac{1}{X_{1,4}X_{5,10}X_{6,9}} + \frac{1}{X_{3,6}X_{2,7}X_{1,8}} + \frac{1}{X_{5,8}X_{4,9}X_{3,10}} + \frac{1}{X_{7,10}X_{1,6}X_{2,5}} + \frac{1}{X_{2,9}X_{3,8}X_{4,7}} \\
& + \frac{1}{X_{1,4}X_{1,8}X_{5,8}} + \frac{1}{X_{3,6}X_{3,10}X_{7,10}} + \frac{1}{X_{5,8}X_{2,5}X_{2,9}} + \frac{1}{X_{7,10}X_{4,7}X_{1,4}} + \frac{1}{X_{2,9}X_{6,9}X_{3,6}} \\
& + \frac{1}{X_{1,8}X_{5,8}X_{2,5}} + \frac{1}{X_{3,10}X_{7,10}X_{4,7}} + \frac{1}{X_{2,5}X_{2,9}X_{6,9}} + \frac{1}{X_{4,7}X_{1,4}X_{1,8}} + \frac{1}{X_{6,9}X_{3,6}X_{3,10}}. \quad (60)
\end{aligned}$$

**Example 7** (Quintic theory). The first non-trivial case in a quintic theory with potential  $V(\phi) = \lambda_5\phi^5$  is  $N = 11$  with  $n = 3$  and  $\Lambda = (3, 3, 3)$ . The mesh for this case is

$$\begin{array}{ccccccccc}
& (1, 8) & & (4, 11) & & (3, 7) & & (6, 10) & & (2, 9) & & (1, 5) \\
& \nearrow & \searrow & \nearrow & \searrow & \nearrow & \searrow & \nearrow & \searrow & \nearrow & \searrow & \nearrow & \searrow \\
(1, 5) & & (4, 8) & & (7, 11) & & (3, 10) & & (2, 6) & & (5, 9) & & (1, 8)
\end{array} \quad (61)$$

matching the 3-cluster category  $\mathcal{C}_{A_2}^3$  in (46). The scattering amplitude is given as 22 terms obtained in terms of the projectives marked in Fig. 13 using the correspondence between



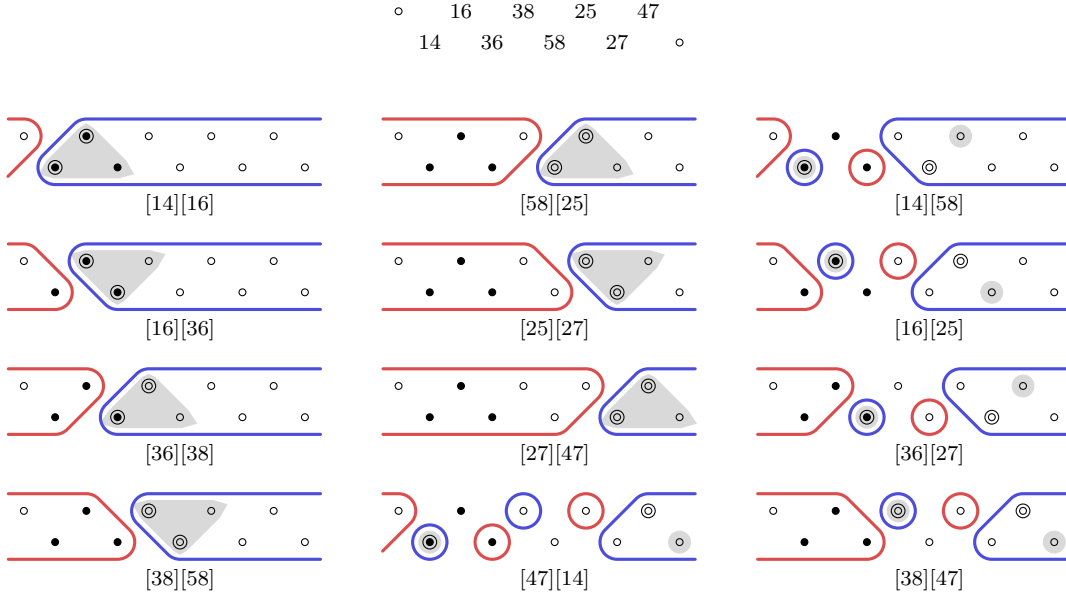


Figure 14: The twelve 2-intermediate  $t$ -structures of  $\mathcal{D}_{A_2}$ , their hearts (shaded), projective objects (circled vertices) and their contribution to the scattering amplitude

planar variables in (61) and the representations in (46) as

$$\begin{aligned}
S_{11}(\phi^5) = & \frac{1}{X_{1,5}X_{1,8}} + \frac{1}{X_{1,8}X_{4,8}} + \frac{1}{X_{4,8}X_{4,11}} + \frac{1}{X_{4,11}X_{7,11}} + \frac{1}{X_{7,11}X_{3,7}} + \frac{1}{X_{3,7}X_{3,10}} \\
& + \frac{1}{X_{3,10}X_{6,10}} + \frac{1}{X_{6,10}X_{2,6}} + \frac{1}{X_{2,6}X_{2,9}} + \frac{1}{X_{2,9}X_{5,9}} + \frac{1}{X_{1,5}X_{7,11}} + \frac{1}{X_{1,8}X_{3,7}} \\
& + \frac{1}{X_{4,8}X_{3,10}} + \frac{1}{X_{4,11}X_{6,10}} + \frac{1}{X_{7,10}X_{2,6}} + \frac{1}{X_{3,7}X_{2,9}} + \frac{1}{X_{3,10}X_{5,9}} + \frac{1}{X_{1,5}X_{6,10}} \\
& + \frac{1}{X_{1,8}X_{2,6}} + \frac{1}{X_{4,8}X_{2,9}} + \frac{1}{X_{4,11}X_{5,9}} + \frac{1}{X_{1,5}X_{5,9}}. \quad (62)
\end{aligned}$$

## 4.1 General potentials

As mentioned earlier, the description of the category arising in the computation of scattering amplitudes for theories with general polynomial potentials (1) with more than one terms is more involved. In terms of planar polygons the angulations are now effected by smaller polygons of different number of edges at once, specifically, with  $n_i$  number of  $m_i$ -gons. We refer to it as a mixed angulation. This makes the enumeration of angulations cumbersome. While still less straightforward than the previous cases with equal  $m_i$ 's, we present a method to write the scattering amplitudes using the category theoretic paraphernalia which can be developed into a computer code.

The procedure to obtain the mesh diagram described in (22) and exemplified in (30) using the partition  $\Lambda$  yields the pseudo-periodic category described in section 3.4. For an  $N$ -particle scattering with potential (1) the pseudo-periodic category is modelled on the



in Fig. 12. The projectives  $[1, 3] - [1, 4] - [4, 6]$  may be obtained from the first one by replacing  $[1, 5]$  by  $[4, 6]$ . We thus have the grading  $\circ - [1, 3] - [1, 4] - [4, 6] - \circ$ , where we have also appended the null entries. From it using the permutations of  $\Lambda$  to select projectives we obtain

$$\circ \begin{array}{c} \xrightarrow{\text{red}} 1,3 \xrightarrow{\text{blue}} 1,4 \xrightarrow{\text{red}} 4,6 \xrightarrow{\text{blue}} \circ \\ \xrightarrow{\text{green}} \end{array} \quad (65)$$

This furnishes two further sets, namely,  $[1, 3], [4, 6]$  and  $[1, 4], [4, 6]$  of projectives and hence two more terms to the scattering amplitude. The repeated set  $[1, 3], [1, 4]$  is not to be counted again. As a third example, let us consider the thirteenth diagram in Fig. 12. The set of projectives  $\circ - [1, 3] - [3, 5] - [1, 5] - \circ$  is obtained again from the first one, by replacing  $[1, 4]$  by  $[3, 5]$ . The choice of projectives for the pseudo-periodic quiver is

$$\circ \begin{array}{c} \xrightarrow{\text{red}} 1,3 \xrightarrow{\text{blue}} 3,5 \xrightarrow{\text{red}} 1,5 \xrightarrow{\text{blue}} \circ \\ \xrightarrow{\text{green}} \end{array} \quad (66)$$

This yields yet two more sets of projectives, namely,  $[1, 3], [3, 5]$  and  $[3, 5], [1, 5]$ . Proceeding in this manner we obtain all the sets of projectives of hearts of intermediate  $t$ -structures of the pseudo-periodic orbit category. The resulting scattering amplitude is [11]

$$\begin{aligned} S_6(\phi^3 + \phi^4) = & \frac{1}{X_{1,3}X_{1,4}} + \frac{1}{X_{1,3}X_{1,5}} + \frac{1}{X_{1,3}X_{3,5}} + \frac{1}{X_{1,3}X_{3,6}} + \frac{1}{X_{1,3}X_{4,6}} + \frac{1}{X_{1,4}X_{1,5}} \\ & + \frac{1}{X_{1,4}X_{2,4}} + \frac{1}{X_{1,4}X_{4,6}} + \frac{1}{X_{1,5}X_{2,4}} + \frac{1}{X_{1,5}X_{2,5}} + \frac{1}{X_{1,5}X_{3,5}} + \frac{1}{X_{2,4}X_{2,5}} \\ & + \frac{1}{X_{2,4}X_{2,6}} + \frac{1}{X_{2,4}X_{4,6}} + \frac{1}{X_{2,5}X_{2,6}} + \frac{1}{X_{2,5}X_{3,5}} + \frac{1}{X_{2,6}X_{3,5}} + \frac{1}{X_{2,6}X_{3,6}} \\ & + \frac{1}{X_{2,6}X_{4,6}} + \frac{1}{X_{3,5}X_{3,6}} + \frac{1}{X_{3,6}X_{4,6}}. \quad (67) \end{aligned}$$

Two cases arise for  $N = 7$ . The mesh diagrams (68) and (70) are the pseudo-periodic categories corresponding to the periodic categories  $\mathcal{P}_{A_2}^7$  given in (51) and  $\mathcal{P}_{A_3}^7$ , given in (53), respectively. The mesh diagram for  $N = 7$  with  $\Lambda = (1, 2, 2)$  is

$$\begin{array}{cccccccccccc} & 1,5 & 2,7 & 1,4 & 3,6 & 5,7 & 2,6 & 1,4 & 3,5 & 4,7 & 2,6 & 1,3 \\ \nearrow & \searrow & \nearrow & \searrow & \nearrow & \searrow & \nearrow & \searrow & \nearrow & \searrow & \nearrow & \searrow \\ 1,3 & 2,5 & 4,7 & 1,6 & 3,7 & 2,5 & 4,6 & 1,5 & 3,7 & 2,4 & 3,6 & 1,5 \end{array} \quad (68)$$

The scattering amplitude is obtained by starting with the cluster category of an  $A_4$  quiver. It has terms with two  $X$ 's in the denominator, for example,  $\frac{1}{X_{1,3}X_{1,5}}$ .

$$(69)$$



For  $N = 12$  and Feynman diagrams with  $n = 4$  vertices, two quartic and two quintic, the mesh is the pseudo-periodic category (76) corresponding to (75). The scattering amplitude can be obtained starting with the cluster category of an  $A_9$  quiver.

As the last example, let us consider scattering with a potential with three terms.

**Example 10** ((3, 4, 5) theory). For  $V(\phi) = \lambda_3\phi^3 + \lambda_4\phi^4 + \lambda_5\phi^5$  the mesh for  $N = 8$  and three vertices, one each of cubic, quartic and quintic ones, the mesh is the pseudo-periodic category

$$\begin{array}{cccccccccccccccc}
 & 1,5 & 2,8 & 1,4 & 3,7 & 6,8 & 2,7 & 1,5 & 4,6 & 5,8 & 3,7 & 2,4 & 3,6 & 1,5 \\
 & \nearrow & \searrow & \nearrow & \searrow & \nearrow & \searrow & \nearrow & \searrow & \nearrow & \searrow & \nearrow & \searrow & \nearrow \\
 1,3 & 2,5 & 4,8 & 1,7 & 3,8 & 2,6 & 5,7 & 1,6 & 4,8 & 3,5 & 4,7 & 2,6 & 1,3 & 
 \end{array} \tag{73}$$

The scattering amplitude

$$\begin{aligned}
 S_8(\phi^3 + \phi^4 + \phi^5) = & \frac{1}{X_{1,3}X_{1,5}} + \frac{1}{X_{2,4}X_{2,6}} + \frac{1}{X_{3,5}X_{3,7}} + \frac{1}{X_{4,6}X_{4,8}} + \frac{1}{X_{5,7}X_{1,5}} + \frac{1}{X_{6,8}X_{2,6}} \\
 & + \frac{1}{X_{1,7}X_{3,7}} + \frac{1}{X_{2,8}X_{4,8}} + \frac{1}{X_{1,3}X_{4,8}} + \frac{1}{X_{2,4}X_{1,5}} + \frac{1}{X_{3,5}X_{2,6}} + \frac{1}{X_{4,6}X_{3,7}} \\
 & + \frac{1}{X_{5,7}X_{4,8}} + \frac{1}{X_{6,8}X_{1,5}} + \frac{1}{X_{1,7}X_{2,6}} + \frac{1}{X_{2,8}X_{3,7}} + \frac{1}{X_{1,3}X_{3,7}} + \frac{1}{X_{2,4}X_{4,8}} \\
 & + \frac{1}{X_{3,5}X_{1,5}} + \frac{1}{X_{4,6}X_{2,6}} + \frac{1}{X_{5,7}X_{3,7}} + \frac{1}{X_{6,8}X_{4,8}} + \frac{1}{X_{1,7}X_{1,5}} + \frac{1}{X_{2,8}X_{2,6}} \\
 & + \frac{1}{X_{2,5}X_{2,8}} + \frac{1}{X_{3,6}X_{1,3}} + \frac{1}{X_{4,7}X_{2,4}} + \frac{1}{X_{5,8}X_{3,5}} + \frac{1}{X_{1,6}X_{4,6}} + \frac{1}{X_{2,7}X_{5,7}} \\
 & + \frac{1}{X_{3,8}X_{6,8}} + \frac{1}{X_{1,4}X_{1,7}} + \frac{1}{X_{2,5}X_{1,7}} + \frac{1}{X_{3,6}X_{2,8}} + \frac{1}{X_{4,7}X_{1,3}} + \frac{1}{X_{5,8}X_{2,4}} \\
 & + \frac{1}{X_{1,6}X_{3,5}} + \frac{1}{X_{2,7}X_{4,6}} + \frac{1}{X_{3,8}X_{5,7}} + \frac{1}{X_{1,4}X_{6,8}} + \frac{1}{X_{2,5}X_{6,8}} + \frac{1}{X_{3,6}X_{1,7}} \\
 & + \frac{1}{X_{4,7}X_{2,8}} + \frac{1}{X_{5,8}X_{1,3}} + \frac{1}{X_{1,6}X_{2,4}} + \frac{1}{X_{2,7}X_{3,5}} + \frac{1}{X_{3,8}X_{4,6}} + \frac{1}{X_{1,4}X_{5,7}} \\
 & + \frac{1}{X_{2,5}X_{5,7}} + \frac{1}{X_{3,6}X_{6,8}} + \frac{1}{X_{4,7}X_{1,7}} + \frac{1}{X_{5,8}X_{2,8}} + \frac{1}{X_{1,6}X_{1,3}} + \frac{1}{X_{2,7}X_{2,4}} \\
 & + \frac{1}{X_{3,8}X_{3,5}} + \frac{1}{X_{1,4}X_{4,6}} + \frac{1}{X_{4,8}X_{1,4}} + \frac{1}{X_{1,5}X_{2,5}} + \frac{1}{X_{2,6}X_{3,6}} + \frac{1}{X_{3,7}X_{4,7}} \\
 & + \frac{1}{X_{4,8}X_{5,8}} + \frac{1}{X_{1,5}X_{1,6}} + \frac{1}{X_{2,6}X_{2,7}} + \frac{1}{X_{3,7}X_{3,8}} + \frac{1}{X_{4,8}X_{3,8}} + \frac{1}{X_{1,5}X_{1,4}} \\
 & + \frac{1}{X_{2,6}X_{2,5}} + \frac{1}{X_{3,7}X_{3,6}} + \frac{1}{X_{4,8}X_{4,7}} + \frac{1}{X_{1,5}X_{5,8}} + \frac{1}{X_{2,6}X_{1,6}} + \frac{1}{X_{3,7}X_{2,7}}
 \end{aligned} \tag{74}$$

is obtained from the cluster category of an  $A_5$  quiver with the projectives chosen using  $\Lambda = (1, 2, 3)$ .

## 5 Summary

To conclude, in this article we obtain a method to write down the scattering amplitudes of scalar field theories with any polynomial potential (1) in a categorical framework, generalizing the case of cubic theory [15]. One important advantage of the approach is in bookkeeping and hence the algorithm presented can be developed into a code. The description is in terms of certain triangulated categories of representations of quivers of type  $A$ . Planar Feynman diagrams of scalar theories with potential (1) are dual to subdivisions of polygons. The latter is known to be associated to (higher) cluster categories of quivers of type  $A$ . We show that the terms of the scattering amplitude of  $N$  particles in a theory with a single-term potential  $V(\phi) = \lambda\phi^{m+2}$  at an order  $\lambda^n$  are given by the projectives of the hearts of the  $m$ -intermediate  $t$ -structures of  $m$ -cluster category of an  $A_{n-1}$  quiver. The  $m$ -cluster category arises as the mesh diagram obtained in terms of the kinematic planar variables  $X$ . For a generic potential (1) the terms in the scattering amplitude are given by a subset of the projectives of hearts of intermediate  $t$ -structure of the cluster category of an  $A_{N-3}$  quiver. The mesh diagram then is the pseudo-periodic category modelled on the  $N$ -periodic category with extra intermediate identification of the planar variables. It may be possible to view this as a quotient of the triangulated category of the AR quiver by a group of homomorphisms with more than one generators (39).



**Acknowledgements** This collaboration started when the first and last named authors were visiting researchers at the Hausdorff Research Institute for Mathematics in Bonn as part of the Junior Trimester Program “New Trends in Representation Theory” and we would like to thank the institute for the hospitality and the excellent working conditions. S. Barmeier was also supported by the Research Training Group GK1821 “Cohomological Methods in Geometry” at the University of Freiburg funded by the Deutsche Forschungsgemeinschaft (DFG, German Research Foundation). H. Treffinger was partially funded by the DFG under Germany’s Excellence Strategy Programme – EXC-2047/1 – 390685813. H. Treffinger is also supported by the European Union’s Horizon 2020 research and innovation programme under the Marie Skłodowska-Curie grant agreement No 893654. H. Treffinger would also like to thank the Isaac Newton Institute for Mathematical Sciences, Cambridge, for support and hospitality during the programme “Cluster Algebras and Representation Theory” where part of the work on this paper was undertaken. This work was supported by EPSRC grant no EP/K032208/1 and the Simons Foundation.

## References

- [1] N. Arkani-Hamed, Y. Bai, S. He, G. Yan, “Scattering Forms and the Positive Geometry of Kinematics, Color and the Worldsheet”, *JHEP* **05** (2018) 096.
- [2] J. Drummond, J. Foster, Ö. Gürdoğan, C. Kalousios, “Tropical Grassmannians, Cluster Algebras and Scattering Amplitudes”, *JHEP* **04** (2020) 146.
- [3] A. Padrol, Y. Palu, V. Pilaud, P.-G. Plamondon, “Associahedra for finite type cluster algebras and minimal relations between  $g$ -vectors”, arXiv:1906.06861 [math.RT].
- [4] V. Bazier-Matte, G. Douville, K. Mousavand, H. Thomas, E. Yıldırım, “ABHY associahedra and Newton polytopes of  $F$ -polynomials for finite type cluster algebras”, arXiv:1808.09986 [math-RT].
- [5] N. Arkani-Hamed, J. L. Bourjaily, F. Cachazo, A. B. Goncharov, A. Postnikov, J. Trnka, “Scattering amplitudes and the positive Grassmannian”, arXiv:1212.5605 [hep-th].
- [6] P. Banerjee, A. Laddha, P. Raman, “Stokes Polytopes: The positive geometry for  $\phi^4$  interactions”, *JHEP* **08** (2019) 067.
- [7] P. Raman, “The positive geometry for  $\phi^p$  interactions”, *JHEP* **10** (2019) 271.
- [8] R. Kojima, “Weights and recursion relations for  $\phi^p$  tree amplitudes from the positive geometry”, *JHEP* **08** (2020) 054.
- [9] I. Srivastava, “Constraining the weights of Stokes polytopes using BCFW recursions for  $\phi^4$ ”, arXiv:2005.12886 [hep-th].
- [10] P. B. Aneesh, P. Banerjee, M. Jagadale, R. R. John, A. Laddha, S. Mahato, “On positive geometries of quartic interactions II: Stokes polytopes, lower forms on associahedra and worldsheet forms”, *JHEP* **04** (2020) 149.



- [11] P. B. Aneesh, M. Jagadale, N. Kalyanapuram, “Accordiohedra as positive geometries for generic scalar field theories”, *Phys. Rev. D* **100** (2019) 106013.
- [12] M. Jagadale and A. Laddha, “On the positive geometry of quartic interactions III: One loop integrands from polytopes”, arXiv:2007.12145 [hep-th].
- [13] Md. Abhishek, S. Hegde, A. P. Saha, “One-loop integrand from generalised scattering equations”, *JHEP* **05** (2021) 012.
- [14] N. Arkani-Hamed, S. He, G. Salvatori, H. Thomas, “Causal diamonds, cluster polytopes and scattering amplitudes”, arXiv:1912.12948 [hep-th].
- [15] S. Barmeier and K. Ray, “Learning scattering amplitudes by heart”, *Phys. Lett. B* **820** (2021) 136594.
- [16] K. Baur and B. Marsh, “A geometric description of the  $m$ -cluster categories of type  $D_n$ ”, *Int. Math. Res. Not.* (2007) rnm011.
- [17] K. Baur, “Cluster categories,  $m$ -cluster categories and diagonals in polygons”, *Geometric methods in representation theory II*, 261–273, Sémin. Congr. 24-II, Soc. Math. France, Paris, 2012.
- [18] K. Baur and R. J. Marsh, “A geometric description of  $m$ -cluster categories”, *Trans. Amer. Math. Soc.* **360** (2008) 5789.
- [19] B. Keller, “Cluster algebras, quiver representations and triangulated categories”, *Triangulated categories*, 76–160, Cambridge University Press, 2010.
- [20] R. Schiffler, “Quiver representations”, Canadian Mathematical Society, 2010.
- [21] A. B. Buan, R. J. Marsh, M. Reineke, I. Reiten, G. Todorov, “Tilting theory and cluster combinatorics”, *Adv. Math.* **204** (2006) 572.
- [22] T. Adachi, O. Iyama, I. Reiten, “ $\tau$ -tilting theory”, *Compos. Math.* **150** (2014) 415.
- [23] R. P. Thomas, “Derived categories for the working mathematician”, *Winter School on Mirror Symmetry, Vector Bundles and Lagrangian Submanifolds* (Cambridge, MA, 1999), 349–361, American Mathematical Society, Providence, RI, 2001.
- [24] S. Mukhopadhyay and K. Ray, “Branes in hearts with perverse sheaves”, *Indian J. Phys. A* **80** (2006) 1109.
- [25] T. Brüstle, D. Yang, “Ordered exchange graphs”, *Advances in Representation Theory of Algebras*, 135–193, European Mathematical Society, 2013.
- [26] B. Keller, “On triangulated orbit categories”, *Doc. Math.* **10** (2005) 551.
- [27] S. Saito, “Tilting objects in periodic triangulated categories”, arXiv:2011.14096 [math.RT].
- [28] A. B. Buan, I. Reiten, H. Thomas, “Three kinds of mutation”, *J. Algebra* **339** (2011) 97.